Environmental Modelling & Software 84 (2016) 263–289

Contents lists available at ScienceDirect

Environmental Modelling & Software

journal homepage: www.elsevier.com/locate/envsoft

An enhanced SWAT wetland module to quantify hydraulic interactions between riparian depressional wetlands, rivers and aquifers

Mohammed M. Rahman*, Julian R. Thompson, Roger J. Flower

Wetland Research Unit, UCL Department of Geography, University College London, Gower Street, London, WC1E 6BT, UK

ARTICLE INFO

Article history:
Received 24 October 2015
Received in revised form
30 June 2016
Accepted 1 July 2016
Available online 15 July 2016

Keywords:
Riparian wetland
River
Groundwater
Interaction
SWAT

ABSTRACT

This study develops a modified version of the Soil and Water Assessment Tool (SWAT) designed to better represent riparian depressional wetlands (SWATrw). It replaces existing unidirectional hydrological interactions between a wetland and a river/aquifer with a more robust bidirectional approach based on hydraulic principles. SWATrw incorporates a more flexible wetland morphometric formula and a connecting channel concept to model wetland-river interactions. SWAT and SWATrw were tested for the Barak-Kushiyara River Basin (Bangladesh and India). Although the two models showed small differences in simulated stream flow, SWATrw outperformed SWAT in reproducing river stages and the pre-monsoon river-spills into riparian wetlands. SWATrw showed that the observed presence of dry season water in the wetland was due to reduced seepage to the local groundwater table whilst continuous seepage simulated by SWAT resulted in the wetland drying out completely. The new model therefore more closely simulates the hydrological interactions between wetlands, rivers and groundwater.

© 2016 The Authors. Published by Elsevier Ltd. This is an open access article under the CC BY license (http://creativecommons.org/licenses/by/4.0/).

Software availability:

Name of software: SWAT2012 (Soil and Water Assessment Tool)
Developer: USDA Agricultural Research Service (USDA-ARS) and Texas A&M AgriLife Research
Contact address: 808 E Blackland Rd, Temple, TX 76502, United States,
Phone: +1 254-770-650; http://blackland.tamu.edu/models/swat/
Year first available: 2012
Hardware required: PC
Software required: ArcGIS
Program language: FORTRAN
Program size: 3.1 MB
Availability and cost: Freely available at http://swat.tamu.edu/software/swat-executables/. Both compiled version and source code of the modified model presented in this paper (SWATrw) can be provided upon request to the corresponding author.

1. Introduction

Wetlands are widely recognised as important habitats for a wide range of plants and animals as well as providing benefits to people through hydrological, biological and chemical functions (Bengtson and Padmanabhan, 1999; Frohn et al., 2012; Hattermann et al., 2008, 2006; Junk et al., 2013; Kadlec and Wallace, 2009; Kulawardhana et al., 2007). The functions related to wetland hydrological processes are amongst the most frequently and intensively studied (Bullock and Acreman, 2003; Heimann and Krempa, 2011; Lindsay et al., 2004; Mendoza-Sanchez et al., 2013; Phan et al., 2011; Thompson, 2004; Wu and Johnston, 2008). Hydrological characteristics exert a dominant role in determining wetland ecological conditions whilst the presence of wetlands within a catchment impacts downstream flow regimes (Bullock and Acreman, 2003; Golden et al., 2014; Heimann and Krempa, 2011; Karim et al., 2012; Krause et al., 2007; Lindsay et al., 2004; Wu and Johnston, 2008) as well as influencing groundwater systems (Golden et al., 2014; Kazezyılmaz-Alhan et al., 2007; Min et al., 2010; Restrepo et al., 1998; Thompson et al., 2004). At the catchment-scale, wetlands are commonly thought of as potentially providing a buffer storage which can retain runoff during wet periods and in turn attenuate peak flows further downstream (Craft and Casey, 2000; Hattermann et al., 2008; Heimann and Krempa, 2011; Kulawardhana et al., 2007; Smith et al., 1995). However,

* Corresponding author.
E-mail address: mohammed.rahman.12@ucl.ac.uk (M.M. Rahman).

http://dx.doi.org/10.1016/j.envsoft.2016.07.003
1364-8152/© 2016 The Authors. Published by Elsevier Ltd. This is an open access article under the CC BY license (http://creativecommons.org/licenses/by/4.0/).

this supposed flow reduction ability is not equally applicable to all wetlands and is influenced by factors that include the location of wetlands within a catchment, their geometry and storage capacity, antecedent storage and the nature and degree of hydraulic connectivity with adjacent water bodies such as rivers and underlying aquifers. For example, a geographically isolated wetland (GIW) which is completely surrounded by upland areas to form a depressional system (Golden et al., 2014) can have strong interactions with underlying groundwater systems depending on the hydraulic properties of the underlying substrate (Fan and Miguez-Macho, 2011; Golden et al., 2014; Hollis and Thompson, 1998; Pyzoha et al., 2008; Restrepo et al., 1998). However, if the wetland is poorly connected with local river systems, it will have negligible influences on downstream flows compared to a riparian wetland in close hydraulic contact with a river channel (Ogawa and Male, 1986; Sun et al., 2004). As a result of this interaction with other water bodies riparian wetlands generally exhibit more complex hydrological behaviour than GIWs with inflows from rivers and runoff from upland areas occurring more rapidly than groundwater exchanges (Walton et al., 1996).

Hydrological/hydraulic interactions between wetlands, other water bodies and aquifers can potentially be assessed through in-situ monitoring. This is particularly valuable in relatively small sites where interactions among hydrological processes are relatively tractable over small spatial scales (e.g. Clilverd et al., 2013). However, instrumenting much larger catchments which might contain many wetlands is frequently impractical (Kite and Droogers, 2000; Krasnostein and Oldham, 2004). Hydrological/hydraulic modelling is an alternative approach for large wetlands and catchment-wide studies of the influence of wetlands on hydrological processes. Wetland processes are either directly incorporated in, or have been indirectly modelled by, many catchment models including SWAT (Arnold et al., 1993), SWIM (Hattermann et al., 2008; Krysanova et al., 2005), WATFLOOD (Kouwen, 2013, 1988), MIKE SHE (DHI, 2009), MODFLOW (McDonald and Harbaugh, 1988; Restrepo et al., 1998), FLATWOODS (Sun et al., 1998) and SLURP (Kite, 2001).

There are many different types of catchment hydrological model ranging from those which employ conceptual, lumped approaches to physics-based, fully distributed models (Refsgaard, 1996; Singh, 1995). Regardless of model type, a wetland is commonly considered to be a depressional type landscape feature with an outflow determined by its temporally varying water storage (Kazezyılmaz-Alhan et al., 2007; Kouwen, 2013; Krasnostein and Oldham, 2004; Neitsch et al., 2011; Powell et al., 2008; Walton et al., 1996; Wen et al., 2013). In many fully distributed models, where the model domain is discretised into a number of grids, modelling of depressional (GIW) wetlands can be difficult (Thompson et al., 2004). Golden et al. (2014) suggested that in such cases model grid size could be as large as a wetland's maximum areal extent. This approach is, however, problematical for catchments that contain many wetlands of varying size. Although a finer model grid might enable representation of such a catchment's wetlands, it will impose progressively larger computational costs as the grid size is reduced (Karim et al., 2012; Tucker et al., 2001). An alternative method that avoids this problem is to represent wetlands within a separate conceptual model (Kazezyılmaz-Alhan et al., 2007; Mansell et al., 2000; Singh, 2010; Wen et al., 2013). In this case, hydrological components such as overland flow, interflow, groundwater flow and channel flow in the surrounding uplands are firstly simulated by a catchment model. These are then used to simulate hydrological exchanges to a conceptual wetland model. Unlike fully-distributed models, semi-distributed models (e.g. SWAT, WATFLOOD, SLURP) need not strictly preserve the spatial location of each constituent grid. Instead, homogeneous grids are grouped into a single Hydrologic Response Unit (HRU) or Grouped Response Unit (GRU) (Arnold et al., 2010; Kouwen, 2013). Grids lying within a series of wetlands within a defined area such as a sub-catchment can be assigned to a single wetland HRU/GRU (Arnold et al., 2010; Bingeman et al., 2006; Feng et al., 2012; Golden et al., 2014; Hattermann et al., 2008; Jing and Chen, 2011; Kouwen, 2013; Markstrom et al., 2008). This reduces computational cost and addresses some of the spatial conformity problems that can impact fully-distributed models.

In contrast to GIWs, representation of riparian wetlands in a distributed model can be simplified by assuming they are a part of the river or floodplain (Wen et al., 2013). Riparian wetlands traversed by main rivers can be termed on-channel wetlands whilst off-channel wetlands are bypassed by the main rivers but are located on the floodplain. An on-channel wetland can be modelled as a component reach or storage node within the modelled river system (Jaber and Shukla, 2012, 2005; Martinez-Martinez et al., 2014; Wen et al., 2013). An off-channel wetland can be simulated as a depressional wetland linked to the river by a connecting channel.

Many wetland hydrological models rely on volume-area-depth relationships which are, in turn, controlled by wetland geometry (Hayashi and van der Kamp, 2000; Nilsson et al., 2008). Improperly specified wetland geometry will affect simulated hydrological processes and water levels (Baker et al., 2006; Mansell et al., 2000). As described above, within fully-distributed models representation of wetland geometry relies on a model's grid size and the vertical accuracy of digital elevation data. For semi-distributed or conceptual lumped models, wetland geometry is usually expressed by empirical power equations describing the relationships between volume, area, and depth. This approach is employed in a number of hydrological models including SWAT, WETSIM and WETLANDSCAPE (Johnson et al., 2010). Empirical wetland morphometric equations can be embedded in catchment models and used flexibly for representing wetlands of variable geometry by calibrating scale and shape parameters. Wang et al. (2008) demonstrated this approach in the representation of multiple depression wetlands in the State of Minnesota, USA as a single “Hydrologic Equivalent Wetland” (HEW). Where the precise spatial distribution of wetlands is less important than their hydrological impacts on the catchment water balance, the HEW concept can reduce computational cost of distributed models.

Hydrological interactions of wetlands with aquifers may be simulated as unidirectional or bidirectional (Krause et al., 2007). For example, in MODFLOW, the direction and mass exchange rates between groundwater and surface water (wetland or river) are determined from a hydraulic gradient based leakage equation (Krause et al., 2007; Restrepo et al., 1998). This exchange can occur bidirectionally depending upon relative water levels. In contrast, SWAT's wetland-groundwater interaction is only represented as downward seepage. Golden et al. (2014) reviewed the usability and limitations of some frequently used catchment models in emulating wetland-groundwater interactions. To avoid complexity, many models assume that the residual of the wetland water balance provides an estimate of wetland-groundwater interaction (Chen and Zhao, 2011; Kouwen, 2013; Krasnostein and Oldham, 2004). Others adopt a simplified Darcy's leakage formula (Kazezyılmaz-Alhan et al., 2007; Mendoza-Sanchez et al., 2013; Restrepo et al., 1998; Sophocleous, 2002; Walton et al., 1996; Wilsnack et al., 2001). Flow is generally assumed to occur vertically through the wetted interface separating wetland and aquifer. However, when the water table is very close to the wetland bed, wetland-groundwater interaction will be dominated by horizontal flow (Bouwer, 2002). In such situations, the Dupuit-Forchheimer or Darcy's horizontal groundwater flow equation may be more

appropriate (Min et al., 2010; Sun et al., 1998). For example, the modified SWAT-Landscape Unit (SWAT-LU) model (Sun et al., 2015) employed Darcy's equation to represent horizontal hydraulic interactions between a river and an aquifer beneath a floodplain. However, this model excludes impacts of riparian wetlands, if present, on catchment hydrology.

In representing wetland-river interactions involving GIWs, many models assume that the wetland can discharge into a river but cannot receive overbank flows from it. In such models, the volume of water (or water level elevation) in a wetland and its corresponding threshold value (predominantly controlled by outlet elevation) are the prime determinants of wetland outflow (Feng et al., 2012; Hammer and Kadlec, 1986; Johnson et al., 2010; Kadlec and Wallace, 2009; Powell et al., 2008; Voldseth et al., 2007; Wen et al., 2013; Zhang and Mitsch, 2005). However, in regions characterised by widespread riparian wetlands that are hydraulically connected with adjacent rivers, wetland-river interaction is likely to be bidirectional. Such interactions should be quantified according to hydraulic principles involving relative river and wetland water level elevations as well as the properties of the connection between the two (Kouwen, 2013; Liu et al., 2008; Min et al., 2010; Nyarko, 2007; Restrepo et al., 1998). In the WATFLOOD model, for instance, riparian wetland-river interaction is modelled using the principle of Dupuit-Forchheimer lateral/radial groundwater flow (Kouwen, 2013). Since exchange between riparian wetlands and rivers can occur over the surface and/or through the subsurface, Restrepo et al. (1998) incorporated an equivalent transmissivity expression, obtained for wetland vegetation and the subsurface soil, into the Darcy flow equation of the MODFLOW model.

The Soil and Water Assessment Tool (SWAT), a continuous, conceptual, semi-distributed, catchment scale model (Arnold et al., 1998, 1993; Neitsch et al., 2011), has been employed to simulate a wide range of different river basins (Kushwaha and Jain, 2013; Li et al., 2010; Mishra and Kar, 2012; Spruill et al., 2000; Vazquez-Amábile and Engel, 2005; Wagner et al., 2011). The ability of SWAT to reproduce the hydrology of GIWs has been demonstrated (Javaheri and Babbar-sebens, 2014; Martinez-Martinez et al., 2014; Wang et al., 2008; Wu and Johnston, 2008) but its capability in emulating riparian wetland-river interactions has been relatively under-studied. Liu et al. (2008) did replace the original hydrological routing algorithm in SWAT's wetland module with more robust hydraulic routing as well as incorporating lateral subsurface wetland-river interactions. These modifications improved simulation performance of flow and sediment discharges in a Canadian river basin that included significant coverage of riparian wetlands.

Despite the utility of this enhanced SWAT wetland algorithm, several shortcomings remain. Although the direction of wetland-river exchange is determined from the relative hydraulic head, lateral surface exchange rates are still based on the hydrological routing (i.e. volume basis) of the original SWAT model. Secondly, the wetland volume-area-depth relationship is site specific rather than taking a generalised form that would enable its wider applicability. Thirdly, the hydraulic head independency on downward seepage means that wetland-groundwater exchange does not represent bidirectional wetland-groundwater interaction. These issues are likely to impact SWAT performance in catchments with many riparian wetlands in which wetland-groundwater-river interactions exert a strong influence upon hydrological functioning. The objectives of the current study are therefore to develop a new wetland module for SWAT that can simulate hydraulic interactions between rivers, riparian wetlands and aquifers and to compare the ability of original and modified SWAT models in reproducing the complex wetland-groundwater-river interactions in the Barak-Kushiyara River Basin, a transboundary catchment shared by India and Bangladesh.

2. Methods

2.1. A structural overview of the SWAT model

This study employed the 627th version of SWAT (rev. 627). The current section provides a brief overview of SWAT before focussing on its representation of wetlands. SWAT discretises a river basin into smaller sub-basins each containing one river reach or main channel. Each sub-basin is further divided into HRUs based on unique combinations of land use, soil and surface slope. Different hydrological components (interception, surface runoff, infiltration, evapotranspiration, interflow, groundwater flow, soil moisture storage) are computed at the HRU-scale for a specified time step (e.g. hour, day). An HRU-level hydrological component is related to a time constant parameter (e.g. SURLAG for surface runoff, ALPHA_BF for baseflow) in order to route that component to the main channel of the sub-basin. Results for each component calculated for the different HRUs are summed to provide a sub-basin total. The water yield from a sub-basin is the total amount of surface runoff, lateral flow, and groundwater flow simulated from all the HRUs in the sub-basin in a given time step.

The river or main channel within a sub-basin is generally assumed to have a trapezoidal cross section with a side slope of 1/2. A symmetrical floodplain (side slope = 1/4, bed width = 2 × river mean width) with a bed elevation equivalent to river bank elevation is assumed to run along each side of the river. Two alternative hydrological channel routing methods are available: variable storage and Muskingum. In the former the influence of a channel's hydraulic and physical characteristics (flow depth, cross sectional area, roughness, and slope) on flows is ignored whereas the latter takes these effects into account (Neitsch et al., 2011).

2.2. Wetland simulation in the SWAT model

SWAT incorporates a simple conceptual wetland module. If there are any wetlands in the modelled basin, then the SWAT sub-basins in which they are located must first be identified. The wetland area within each sub-basin area must be specified and can be obtained from digital map data, land use data, topographic maps, or remotely sensed imagery (Baker et al., 2006; Dwivedi et al., 1999; Frohn et al., 2012; Kiesel et al., 2010; Maxa and Bolstad, 2009; Murphy et al., 2007; Rahman et al., 2014). In principle, SWAT allows only one wetland within each sub-basin (Fig. 1). However, if a sub-basin contains more than one wetland, a "Hydrologic Equivalent Wetland" (HEW) can be employed (see Section 1) with its area specified as the total area of all the wetlands within the sub-basin. Like HRUs, wetlands have no real spatial location within a sub-basin. Since the total area of a sub-basin is apportioned among its constituent HRUs, all wetland attributes that affect mass balance, for instance, water surface area and volume, are also proportionally distributed among the HRUs.

Fig. 2 summarises the hydrological interactions in the original SWAT wetland module (as well as the revised wetland module developed in the current study which is discussed below). Unless otherwise stated all equations presented in this paper are for HRU-scale computations although different schematic depictions are drawn at sub-basin scale. The water mass balance equation in SWAT's original wetland module can be written as:

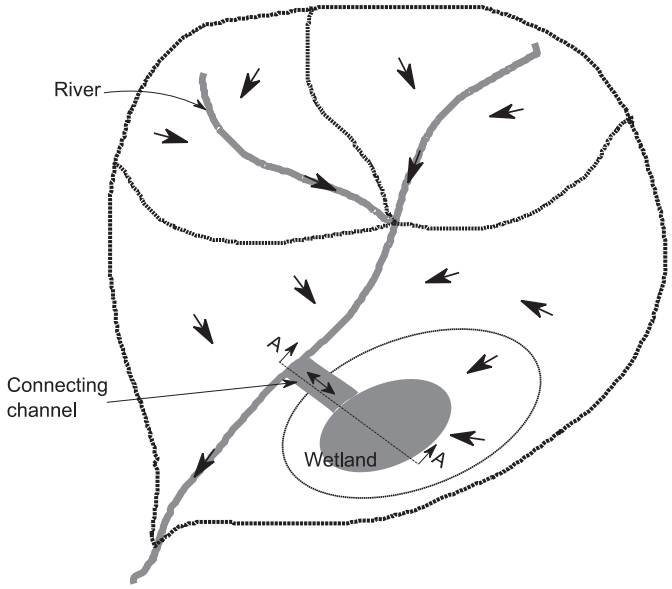

Fig. 1. Graphical representation of a wetland and sub-basin in the SWAT model. The black dotted lines indicate drainage boundaries of sub-basin and wetland and arrow heads indicate direction of overland flow or channel flow. Grey colour represents the extent of water surface in rivers, connecting channels and wetlands.

$$S^{i}_{wet} = S^{i-1}_{wet} + (P + Q_{sur} + Q_{lat})_{wet,in} - (E + Q_{ch\&wet} + Q_{wet\&aq})_{wet,out} \quad (1)$$

where S indicates water storage; P and E are precipitation and evaporation, respectively and $Q_{wet\&aq}$ is the wetland-aquifer exchange which, as discussed above, is unidirectional such that only seepage from the wetland to groundwater is represented. Q_{sur} and Q_{lat} are surface runoff and lateral subsurface or interflow at the HRU-scale, respectively generated from surrounding uplands where the area of these uplands is the difference between total wetland catchment area (upland catchment plus wetland water surface area) and the wetland water surface area. $Q_{ch\&wet}$ is the discharge of water from the wetland to the river (as discussed above, the original wetland module does not represent flows in the opposite direction). The subscripts *wet*, *in*,& *out* indicate wetland, inflow and outflow respectively. The superscript *i* is time step and any absence of this time step notation should be read for current time step. Dimension of each element of the water balance is L^3.

Since the wetland water surface area varies with time due to the net effect of incoming and outgoing fluxes, incoming surface runoff and interflow into a wetland are updated at each time step according to Equation (2):

$$(Q_{sur} + Q_{lat})_{wet,in} = (Q_{sur} + Q_{lat})_{hru} * \left(A_{hru} * wet\_fr - A_{wet}\right) \quad (2)$$

where the subscript *hru* indicates HRU (hydrologic response unit), A_{hru} is the area of an HRU (L^2), *wet_fr* is the fraction of sub-basin area draining into the sub-basin-scale wetland (i.e. the wetland's catchment area), A_{wet} is the wetland's water surface area (L^2) at HRU-scale and other symbols are previously defined. SWAT first estimates surface runoff and interflow without considering any wetland in an HRU. Subsequently the equivalent amount of water, which would have been produced from the area occupied by the HRU-scale wetland (i.e. fraction of total wetland area in an HRU) had it not existed, is deducted from the flows generated across the total HRU area. This is an excellent feature of the SWAT model for a region like that considered in the present study where wetlands are used for seasonal rice cultivation (see Section 2.4) during the dry season. As the flood recedes, the extent of wetlands continuously changes with rice cultivation; thereby, local hydrological processes are also impacted.

The volume of water stored in a wetland is used as an input to an empirical exponential equation in order to calculate the corresponding wetland water surface area:

$$A_{wet} = \beta \cdot S^{\alpha}_{wet} \quad (3)$$

$$\alpha = \frac{\log_{10}(A_{wet,mx}) - \log_{10}(A_{wet,nor})}{\log_{10}(S_{wet,mx}) - \log_{10}(S_{wet,nor})} \quad (4)$$

$$\beta = \frac{A_{wet,mx}}{S^{\alpha}_{wet,mx}} \quad (5)$$

where the coefficients β and α are referred to as the scale factor and shape factors, respectively. $A_{wet,mx}$ and $A_{wet,nor}$ are the wetland water surface areas at maximum and normal capacities of the wetland, respectively. Similarly, $S_{wet,mx}$ and $S_{wet,nor}$ indicate wetland

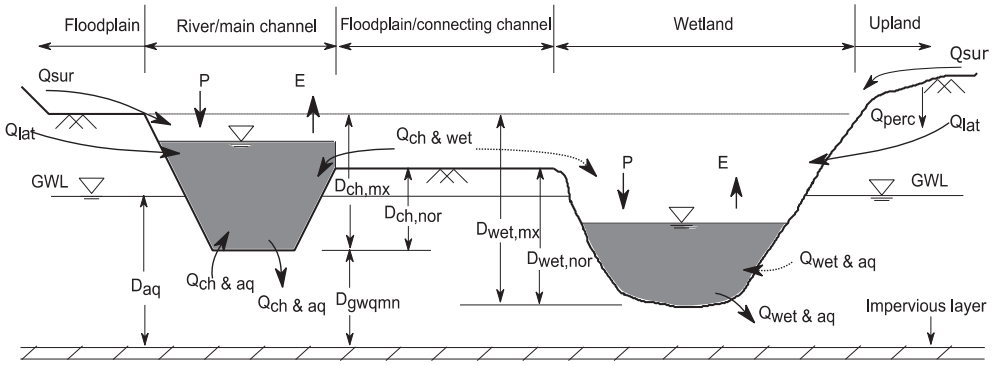

Fig. 2. An example of hydrological interaction, along section A-A (Fig. 1), between a river, riparian wetland and groundwater within SWAT. The extent of wetland shown with the double headed arrow line means the extent at maximum wetland capacity. P = precipitation, E = evaporation, Q_{perc} = percolation, Q_{sur} = surface runoff, Q_{lat} = lateral/inter flow, $Q_{ch\ \&\ aq}$ = exchange between river/main channel and aquifer, $Q_{ch\ \&\ wet}$ = exchange between the river/main channel and wetland, $Q_{wet\ \&\ aq}$ = exchange between the wetland and aquifer either over the floodplain or through the connecting channel, GWL = groundwater level, D_{aq} = height of groundwater level above the aquifer's impervious layer, D_{gwqmn} = height of river's bottom above the aquifer's impervious layer, $D_{ch,mx}$ = maximum channel's depth, $D_{ch,nor}$ = channel's depth from the normal level which is the elevation of river bank at connecting channel, $D_{wet,mx}$ = maximum wetland's depth and $D_{wet,nor}$ = normal depth of wetland. Processes drawn with the dotted lines ($Q_{ch\ \&\ wet}$ and $Q_{wet\ \&\ aq}$) are not currently modelled in SWAT but are included in the SWATrw (SWAT for riparian wetland) model developed in this study.

water volumes at maximum and normal capacities, respectively. The normal wetland capacity is a threshold volume that must be exceeded before the wetland discharges to the river within its sub-basin. For example, in a weir controlled wetland, the normal capacity might be the volume of water that corresponds to the water level reaching the weir crest level. Note that while estimating scale and shape factors (equations (4) and (5) respectively), SWAT uses all necessary wetland inputs for sub-basin-scale wetland and these same factors are subsequently used for all HRU-scale wetlands in the sub-basin. Discharge or surface outflow ($Q_{ch\ \&\ wet}$) from the wetland to the river during a given time step is determined by:

$$Q_{ch\ \&\ wet} = \begin{cases} 0 & if \quad S_{wet} \le S_{wet,nor} \\ \dfrac{S_{wet} - S_{wet,nor}}{10} & if \quad S_{wet,nor} < S_{wet} \le S_{wet,mx} \\ S_{wet} - S_{wet,mx} & if \quad S_{wet} > S_{wet,mx} \end{cases} \tag{6}$$

The unidirectional wetland-groundwater interaction ($Q_{wet\&aq}$) i.e. downward seepage from the wetland is estimated from:

$$Q_{wet\ \&\ aq} = K_{sat} \cdot A_{wet} \tag{7}$$

where K_{sat} is the saturated hydraulic conductivity of the wetland bed (LT^{-1}). The seepage from Equation (7) is routed to the aquifer through an imaginary vadose zone with an exponential decay function (Equation (8)) that gives the wetland's final contribution to aquifer recharge:

$$Q^{i}_{rchrg,aq} = (1 - \delta_{gw}) \cdot Q_{wet\ \&\ aq} + \delta_{gw} \cdot Q^{i-1}_{rchrg,aq} \tag{8}$$

where, $Q^{i}_{rchrg,aq}$ and $Q^{i-1}_{rchrg,aq}$ are the recharge from the wetland (L) to the aquifer at times i and $i-1$, respectively and δ_{gw} is the groundwater delay coefficient. Percolation from the deepest soil layer in the uplands and other seepages (e.g. from rivers and ponds) are also added to $Q_{wet\ \&\ aq}$ to provide the total groundwater recharge from the catchment (given the focus herein on SWAT's wetland module these terms are not detailed). Since wetland-river and wetland-groundwater interactions are the focus of the current study, other wetland processes, for example evaporation, are not elaborated here.

2.3. Wetland simulation in SWATrw

Whilst the wetland module of the current version of SWAT does enable some representation of the hydrological interactions between wetlands and other hydrological components of a river basin, there are, as discussed above, a number of issues that could still be addressed. The following section details the approaches employed in the newly developed SWATrw (SWAT for riparian wetland) model that are designed to improve the representation of the hydrological processes and properties of wetlands.

2.3.1. Wetland volume-area-depth relationship

The empirical equation used in the current SWAT model to represent wetland geometry (Equation (3)) does not explicitly relate depth of water within a wetland with the other two morphometric properties, area and volume. This presents problems where accurate simulation of the wetland water depth is essential, for example in representing hydraulic interactions between wetlands and other water bodies (e.g. rivers and aquifers). Another drawback is the difficulty of establishing appropriate scale and shape parameters. SWAT requires two sets (normal and maximum) of known values for wetland water surface area and volume for inclusion in Equation (4). Estimates of actual wetland water volume are much less frequently available than wetland water surface area. Consequentially, normal and maximum wetland volumes may be established through calibration. This increases uncertainty in the simulation of wetland hydrological functioning. Uncertainty could be reduced by expressing wetland water volume as a function of both wetland water surface area and depth since observations of these two variables are in many cases more readily available. Wetland water surface area can be measured using various techniques including ground survey, aerial photography (Harvey and Hill, 2001), and remotely sensed data (e.g. land use, soil and elevation data) (Baker et al., 2006; Kulawardhana et al., 2007; Lindsay and Creed, 2005; Maxa and Bolstad, 2009; Murphy et al., 2007; Townsend and Walsh, 2001). Wetland water depth at specific locations can be monitored periodically using a range of instrumentation from simple staff gauges to automatic water level recorders. By assuming that wetland side slope is the same as that of the floodplain, Liu et al. (2008) showed that Equation (3) can be related to wetland water depth (D_{wet}) as shown in Equation (9). Nonetheless, the assumption of consistent wetland slope narrows their model's wider applicability particularly in shallow but extensive low-relief wetland systems. Moreover, the compatibility of their wetland model to different wetlands was not reported.

$$D_{wet} = \beta^{-1} \cdot S^{1-\alpha}_{wet} \tag{9}$$

To overcome these limitations, we incorporated a more robust, generalised and flexible wetland geometric formula into SWATrw. This formula was developed by Hayashi and van der Kamp (2000) who tested it for a range of depressional wetlands with non-unique shapes. For the sake of simplicity, their volume-area-depth model is, hereafter, referred to as the H-K wetland morphometry model. The mathematical form of the model as incorporated in SWATrw is shown in equations (10) and (11):

$$A_{wet} = b \cdot \left(\frac{D_{wet}}{D_{wet,0}}\right)^{2/p} \tag{10}$$

$$S_{wet} = \left(\frac{b}{1 + \frac{2}{p}}\right) \cdot \frac{D_{wet}^{\left(1+\frac{2}{p}\right)}}{D_{wet,0}^{\frac{2}{p}}} \tag{11}$$

where b and p are the scale and shape parameters of the model, respectively and $D_{wet,0}$ indicates unit wetland depth. Only the shape parameter has to be calibrated as the scale parameter is calculated from the user specified maximum values of wetland water surface area and depth. Increasing the value of p represents a more cylindrical shaped wetland. One distinguishing feature of the H-K wetland morphometry model is that with only one set of b and p values the model can satisfactorily represent the average geometry of a natural depressional wetland having heterogeneous side slopes (Hayashi and van der Kamp, 2000).

2.3.2. Wetland-river interaction

In this study wetlands are assumed to be on the floodplain but not directly next to the river (see Figs. 1 and 2) in accordance with the riparian off-channel wetlands (see Section 1) that SWATrw is designed to represent. The wetland water level at its maximum capacity is assumed to be the river's highest bank level (i.e. the bed elevation of the intermediate floodplain between the river and the wetland). If a sub-basin contains more than one wetland, then

initially one approximate Hydrologic Equivalent Wetland can be generated by summing maximum water surface areas of each wetland and by averaging the maximum wetland water depths. Nonetheless, a larger variation among wetlands' shape restricts the usability of such a technique.

A riparian wetland can exchange water with the adjacent river according to three processes: (i) overbank flow across the floodplain during periods of high water level (ii) flow through a connecting channel, if one exists, between the river and wetland and (iii) lateral subsurface flow (not considered in this study; see the next paragraph). Although SWAT assumes that the maximum depth of a river within a sub-basin is uniform throughout the river length, this is, in reality, rare. In lowland areas which contain many riparian wetlands the banks of flood-prone rivers are frequently altered by the construction of embankments and dykes designed to reduce the incidence of overbank flows and hence flooding (Clilverd et al., 2013; Gopal, 2013; Junk et al., 2013). High river flows can often breach these dykes at vulnerable sections, for example, at the lowest point of the main river bank where a connecting channel from a riparian wetland joins the river. To model this wetland-river interaction within SWATrw, a connecting channel rather than a floodplain (Figs. 1 and 2) is conceptualised at the vulnerable part of the river bank(s). We think that a simple and flexible channel flow module based on Manning's channel flow equation is appropriate to represent such connectivity. The cross section of a connecting channel is assumed to be rectangular and its width and depth are some fractions of main channel length and maximum depth, respectively and can be established through calibration. When a favourable hydraulic connection is established between a wetland and a river (see below), mass exchange occurs through the connecting channel. The connecting channel has no retention capacity itself but offers resistance to flow due to aquatic vegetation that is common in floodplain/wetland environments. Whilst the assumption of zero retention capacity is considered appropriate for small connecting channels (such as those which characterise the case-study described below and many similar riparian wetland situations), it might not be as equally applicable for larger and longer connecting channels which will have greater surficial and/or sub-surficial (porosity) storage capacity. Unlike SWAT, SWATrw divides a sub-basin river that is connected to a wetland into reach segments whose lengths are proportional to the HRU fractions in the sub-basin containing the wetland (Fig. 3). As a result there is the same number of river reaches as HRUs in a sub-basin. Similarly, the width of a sub-basin connecting channel is also proportioned based on HRU relative extent, and each pair of HRU and river reach sections is associated with the respective downscaled connecting channel. In this way, the largest HRU is paired with the longest river reach and thus the widest connecting channel.

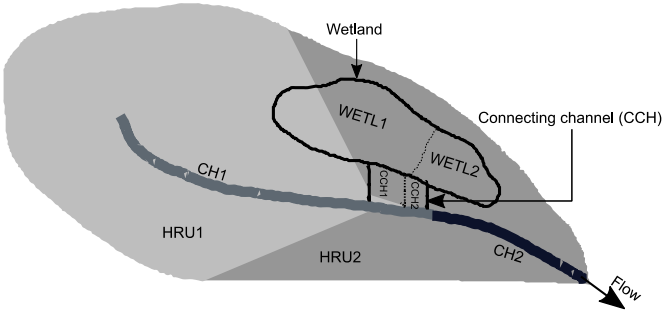

Fig. 3. A hypothetical representation of how SWATrw apportions wetland, main channel and connecting channel among HRUs in a sub-basin. The illustrated sub-basin has two HRUs (shaded light and dark grey). The area of HRU1 (A_{HRU1}) is larger than that of HRU2 (A_{HRU2}). Therefore, the wetland, main channel and associated connecting channel are also disaggregated in such a way so that each of their respective properties (area of wetland, A_{WETL}; width of connecting channel, W_{CCH}; and length of main channel, L_{CH}) has a ratio (A_{WETL1}: A_{WETL2}, W_{CCH1}: W_{CCH1} and L_{CH1}: L_{CH2}) of equalled to A_{HRU1}:A_{HRU2}. During model computation a HRU in a sub-basin is paired with other disaggregated features (wetland, connecting channel and main channel) based on the size of the respective properties.

In SWATrw, wetland-river interaction is assumed to occur only as surface water (i.e. direct lateral subsurface interaction is not considered). Our assumption is that any phreatic or seepage line evolving from a wetland or river will terminate at the intermediate aquifer between them before reaching the river or wetland. This is likely for any single or a combination of the following reasons: low soil permeability, the difference between surface water and groundwater levels is small, and the distance between a wetland and river is large. Hydraulic principles are used to quantify wetland-river interactions. Firstly, the model fixes a datum level against which other elevations such as water levels are referenced. Since the horizontal plane of the wetland water surface at its maximum capacity is assumed to be level with the floodplain (or the highest river bank elevation), a datum of zero elevation is set to either the bed of the river or the wetland depending on which is deeper. Unlike SWAT, the normal threshold depth or normal storage capacity of a wetland is defined by the bed elevation of the connecting channel. The product of a parameter "fraction of maximum river depth at normal level" (CCH_DFR) and maximum river depth ($D_{ch,mx}$) gives the connecting channel's bed height from the river bed, thus the connecting channel's bed is referenced to the datum (wetland or river bed). When both wetland and river water levels fall below the normal level (i.e. the bed of the connecting channel), exchange ceases. When there is a hydraulic head difference between a wetland and a river, and at least one of the water levels is above the normal level, the specific exchange flow rate (flow rate per unit water area) is calculated based on the wetland surface flow equation developed by Kadlec and Wallace (2009):

$$q_{ch\ \&\ wet} = c \cdot d^m \cdot s_f^n \tag{12}$$

where $q_{ch\ \&\ wet}$, d and s_f represent specific exchange flow rate (LT^{-1}), depth of flow (L), and friction slope, respectively. The terms c, m, and n are the conveyance coefficient, depth exponent and slope exponent, respectively. Equation (12) is based on the Manning's channel flow formula ($if c=1/N, m=2/3, n=½$) which was originally developed for turbulent flow. However, evidence from field experiments shows that surface flow over a wetland is most likely laminar or transitional (Hammer and Kadlec, 1986; Kadlec and Wallace, 2009). When applied to a wetland, the value of d in Equation (12) is the mean overland flow depth. However, in our case, the value of d is the depth of flow at the midpoint of the connecting channel and is estimated from Bernoull's energy equation. With reference to Fig. 2, since river water level is above both the normal level (i.e. the bottom of the connecting channel) and wetland water level, flow occurs from the river to the wetland due to the available driving hydraulic head. Flow would be reversed if water levels in the river and the wetland were exchanged. For the example in Fig. 2, the driving hydraulic head is the elevation difference of the river water level and the normal level. Alternatively, if the wetland water level was above the bed of the connecting channel (but still below the river level) the driving hydraulic head would be the difference between the river and wetland water levels. The same principles are applied when wetland water levels are higher than river levels and the direction of exchange is reversed. After simplification of Bernoulli's energy equation, the equation takes the form:

$$d + \frac{1}{2g}\left(c \cdot s_f^n\right)^2 d^{2m} + \left(s_f \cdot \frac{l}{2}\right) - d_{dh} = 0 \quad (13)$$

where l is the length of the connecting channel (L), d_{dh} is the driving hydraulic head (L), and other symbols are previously described. For given values of c, m, n and S_f, the above equation is numerically solved with the Newton-Rapson method.

After calculating the average depth of flow through the connecting channel, the maximum volume of water that can be exchanged during an individual time step is estimated as follows:

$$Q_{ch\ \&\ wet} = (q_{ch\ \&\ wet} \cdot d \cdot w)\Delta t \quad (14)$$

where w is the width of the connecting channel (L) and Δt is the time step (T). Multiplying total river length by the calibration term CCH_LFR (fraction of the river length overflowed at normal elevation) gives the value of w. According to hydraulic principles, flow between two hydraulically connected water reservoirs (here the wetland and river) can continue until their water levels reach the same elevation (or until, in this instance, the water level of the loosing reservoir reaches the bed of the connecting channel). Therefore, if the water volume estimated by Equation (14) is greater than the intake capacity of a receptor reservoir, the actual transferred water volume is re-calculated by reducing the duration of flow time (initially flow time is equal to the model time step) so that water levels reach an equilibrium state. Intake capacity is the volume of water in a receptor reservoir at equilibrium water level less its initial water volume. The necessary mathematical calculations and procedures used in SWATrw to estimate transferable water volume between a wetland and a river are described below. The same procedure is followed for both directions of exchange (i.e. river to wetland and wetland to river).

For the example illustrated in Fig. 2, since the river is in hydraulic connection with the wetland and the water level of the river is higher than that of the wetland, there is clearly a potential discharge into the wetland. For the exchange of a specific volume of water from the river to the wetland, water depths in the loosing river at the end of each time step can be estimated as:

$$\text{Change in water volume } S_{ch}^{t1} - S_{ch}^{t2} = q_{ch\ \&\ wet} \cdot \Delta t \quad (15)$$

$$\left\{W_{bot,ch} \cdot D_{ch}^{t1} + z \cdot \left(D_{ch}^{t1}\right)^2\right\} L_{ch} - \left\{W_{bot,ch} \cdot D_{ch}^{t2} + z \cdot \left(D_{ch}^{t2}\right)^2\right\} L_{ch} = q_{ch\ \&\ wet} \cdot \Delta t \quad (16)$$

$$D_{ch}^{t2} = \frac{-W_{bot,ch} \pm \sqrt{\left(W_{bot,ch}\right)^2 - 4 \cdot z \cdot \left[\frac{(q_{ch\ \&\ wet} \cdot \Delta t)}{L_{ch}} - \left\{W_{bot,ch} \cdot D_{ch}^{t1} + z \cdot \left(D_{ch}^{t1}\right)^2\right\}\right]}}{2 \cdot z} \quad (17)$$

where, S_{ch}^{t1} and S_{ch}^{t2} are the water volumes of the river at time $t1$ and $t2$, D_{ch}^{t1} and D_{ch}^{t2} are the water depths of the river at time $t1$ and $t2$ and $W_{bot,ch}$, L_{ch}, and z are the bottom width, length and side slope of the river (trapezoidal shape), respectively. For the gaining wetland, water levels at the end of each time step can be estimated as:

$$\text{Change in water volume } S_{wet}^{t2} - S_{wet}^{t1} = q_{ch\ \&\ wet} \cdot \Delta t \quad (18)$$

and the combination of equations (11) and (18) gives:

$$D_{wet}^{t2} = \left[\frac{S_{wet}^{t1} + q_{ch\ \&\ wet} \cdot \Delta t}{\left(\frac{b}{b + \frac{2}{p}}\right)} \times D_{wet,0}^{\frac{2}{p}}\right]^{\left(\frac{1}{\left(1+\frac{2}{p}\right)}\right)} \quad (19)$$

where S_{wet}^{t1} and S_{wet}^{t2} are the water volumes of the wetland at time $t1$ and $t2$ and D_{wet}^{t2} is the water depth in the wetland at time $t2$. For the following constraints (Equations (20)–(22)), equations (17) and (19) are solved iteratively by changing the value of Δt. The iteration process starts from the maximum value of Δt (i.e. the time step of the model) and is continued with smaller time steps until a satisfactory solution is achieved. Since the time step in the present modelling study is daily (see below), the maximum number of iterations is set to 142 and the process operates in the chronological order of Equation (23).

$$\frac{(q_{ch\ \&\ wet} \cdot \Delta t)}{L_{ch}} \leq \left\{W_{bot,ch} \cdot D_{ch}^{t1} + z \cdot \left(D_{ch}^{t1}\right)^2\right\} \quad (20)$$

$$D_{ch}^{t2} \geq 0 \text{ and } D_{wet}^{t2} \geq 0 \quad (21)$$

$$\left(E_{ch,bed} + D_{ch}^{t2}\right) \geq \left(E_{wet,bed} + D_{wet}^{t2}\right) \quad (22)$$

$$\left.\begin{array}{c} \Delta t_1,\ \Delta t_1,\ \Delta t_1 \ldots\ldots\ldots \Delta t_{22},\ \Delta t_{23},\ \Delta t_{24} = 24, 23, 22, \ldots\ldots\ldots 3, 2, 1 \text{ (hr)} \\ \Delta t_{25},\ \Delta t_{26},\ \Delta t_{27} \ldots\ldots\ldots \Delta t_{81},\ \Delta t_{82},\ \Delta t_{83} = 59, 58, 57, \ldots\ldots\ldots 3, 2, 1 \text{ (min)} \\ \Delta t_{84},\ \Delta t_{85},\ \Delta t_{86} \ldots\ldots\ldots \Delta t_{140},\ \Delta t_{141},\ \Delta t_{142} = 59, 58, 57, \ldots\ldots\ldots 3, 2, 1 \text{ (sec)} \end{array}\right\} \quad (23)$$

$E_{ch,bed}$ and $E_{wet,bed}$ are the elevations of the river and wetland beds, respectively. Once a solution is attained, the final transferable water volume is re-calculated using Equation (14) for the resultant time step (Δt). Thereafter, storages of water in the wetland and river are updated. A resulting smaller time step than the model's time step (1 day or 24 h) indicates that the receiving water body (i.e. the wetland in the example in Fig. 2) will reach a hydraulic equilibrium state with its delivering waterbody (the river in the example) in less than a whole day. Such a phenomenon can occur where riparian wetlands are rapidly flooded due to a sudden increase in river

discharge (Nishat and Rahman, 2009). Finally if a wetland's water level exceeds its maximum level, which may occur during periods of heavy rainfall over the wetland catchment, all water in excess of the maximum capacity is transferred to the river on the same day, an approach employed in SWAT. This water, in turn, can be simulated as inundating the floodplain if the river exceeds its maximum capacity.

2.3.3. Wetland-groundwater interaction

Application of the current wetland module within SWAT is problematical in situations where bidirectional wetland-groundwater interactions are a common phenomenon. This includes floodplain areas where the groundwater level is very close to the ground surface and fluctuates throughout the year. As indicated in Equation (7), whilst SWAT simulates the seepage of water from a wetland to the underlying aquifer, water from the aquifer does not discharge into the wetland. Moreover, the amount of seepage from a wetland is only controlled by the hydraulic conductivity of the wetland bed material. The role of hydraulic head is completely neglected which is contradictory to the well known Darcy's flow formula. Although a number of past studies have demonstrated SWAT's abilities to model downward wetland-aquifer interactions within North American prairie wetlands where groundwater level seldom crosses the wetland bed level (Wang et al., 2008, 2010), its application is not recommended in situations where bidirectional interactions between a wetland and an aquifer are prevalent (Golden et al., 2014; Sun et al., 2004). This is addressed in SWATrw through the incorporation of a Darcy's flow law based wetland-groundwater interaction algorithm. Initially the elevations of the aquifer bed ($E_{aq,bed}$) and groundwater surface (E_{aq}) are calculated using equations (24) and (25):

$$E_{aq,bed} = E_{ch,bed} - D_{gwqmn} \tag{24}$$

$$E_{aq} = \begin{cases} E_{aq,bed} + D_{aq} & \text{if } D_{aq} \le \left(E_{wet,bed} - E_{aq,bed}\right) \\ E_{aq,bed} + D_{aq} + \left[\dfrac{\left(\dfrac{b}{b+\frac{2}{p}}\right)\cdot\dfrac{D_{wet,aq}^{\left(1+\frac{2}{p}\right)}}{D_{wet,0}^{\frac{2}{p}}}}{A_{hru} - b.\left(\dfrac{D_{wet,aq}}{D_{wet,0}}\right)^{\frac{2}{p}}}\right] & \text{if } D_{aq} > \left(E_{wet,bed} - E_{aq,bed}\right) \\ \text{where, } D_{wet,aq} = D_{aq} - \left(E_{wet,bed} - E_{aq,bed}\right) & \end{cases} \tag{25}$$

In Fig. 2, D_{gwqmn} is illustrated as the height of the channel bed above the aquifer bed which can be determined by dividing the given threshold aquifer water depth to initiate baseflow by the aquifer specific yield. The elevation of channel bed ($E_{ch,bed}$) has already been defined in Section 2.3.2. D_{aq} is the height of groundwater level above the aquifer bed uniformly distributed across the HRU area. The expression within the square brackets of Equation (25) returns an additional groundwater depth to be superimposed over the original SWAT simulated GWL uniformly distributed across the HRU. This is estimated by dividing the water volume that would have been contained in a wetland at GWL had the wetland been filled with the aquifer material, by HRU area less the wetland surface area at GWL. The reason for this arrangement is that SWAT currently assumes that the areal extent of an HRU-scale aquifer, with uniform depth, is the same as that of the HRU. This would underestimate the actual GWL of a shallow aquifer when the GWL rises above the wetland bed (see Fig. 2) because the volume occupied by a depressional wetland is not a part of the aquifer. The total amount of water in an aquifer during a time step is divided by aquifer specific yield (S_y) to obtain the equivalent depth of groundwater in the aquifer (D_{gwqmn} & D_{aq}). Once the elevation of GWL is calculated, SWATrw simulates wetland-groundwater interaction using the following assumptions: (i) if the GWL is below the wetland bed seepage water is routed through a vadose zone to obtain net recharge from the wetland, and (ii) if the GWL is at or above the wetland bed wetland-groundwater interaction is instantaneous i.e. any seepage from the wetland or groundwater flow to the wetland will not be lagged by a time factor. The following equations represent the mathematical formulations of the wetland-groundwater interactions:

$$Q_{wet\,\&\,aq} = \begin{cases} K_{sat}\cdot\dfrac{E_{wet} - E_{wet,bed}}{wet_{th}}\cdot A_{wet} & \text{if } E_{aq} < E_{wet,bed} \\ K_{sat}\cdot\dfrac{E_{wet} - E_{aq}}{wet_{th}}\cdot A_{wet} & \text{if } E_{aq} \le E_{wet} \text{ and } E_{aq} \ge E_{wet,bed} \\ K_{sat}\cdot\dfrac{E_{aq} - E_{wet}}{wet_{th}}\cdot A_{wet,aq} & \text{if } E_{aq} > E_{wet} \text{ and } E_{aq} \ge E_{wet,bed} \end{cases} \tag{26}$$

$$Q_{rchrg,aq}^{i} = \begin{cases} (1-\delta_{gw})\cdot Q_{wet\,\&\,aq} + \delta_{gw}\cdot Q_{rchrg,aq}^{i-1} & \text{if } E_{aq} < E_{wet,bed} \\ Q_{wet\,\&\,aq} + \delta_{gw}\cdot Q_{rchrg,aq}^{i-1} & \text{if } E_{aq} \le E_{wet} \text{ and } E_{aq} \ge E_{wet,bed} \end{cases} \tag{27}$$

where E_{wet}, $A_{wet,aq}$, and wet_{th} represent wetland water level elevation, wetland water surface area at GWL elevation (i.e. when the wetland water depth is $D_{wet,aq}$), the thickness of the wetland bottom (commonly known as hyporheic zone), respectively and other symbols are previously described. After estimating $Q_{wet\ \&\ aq}$, the

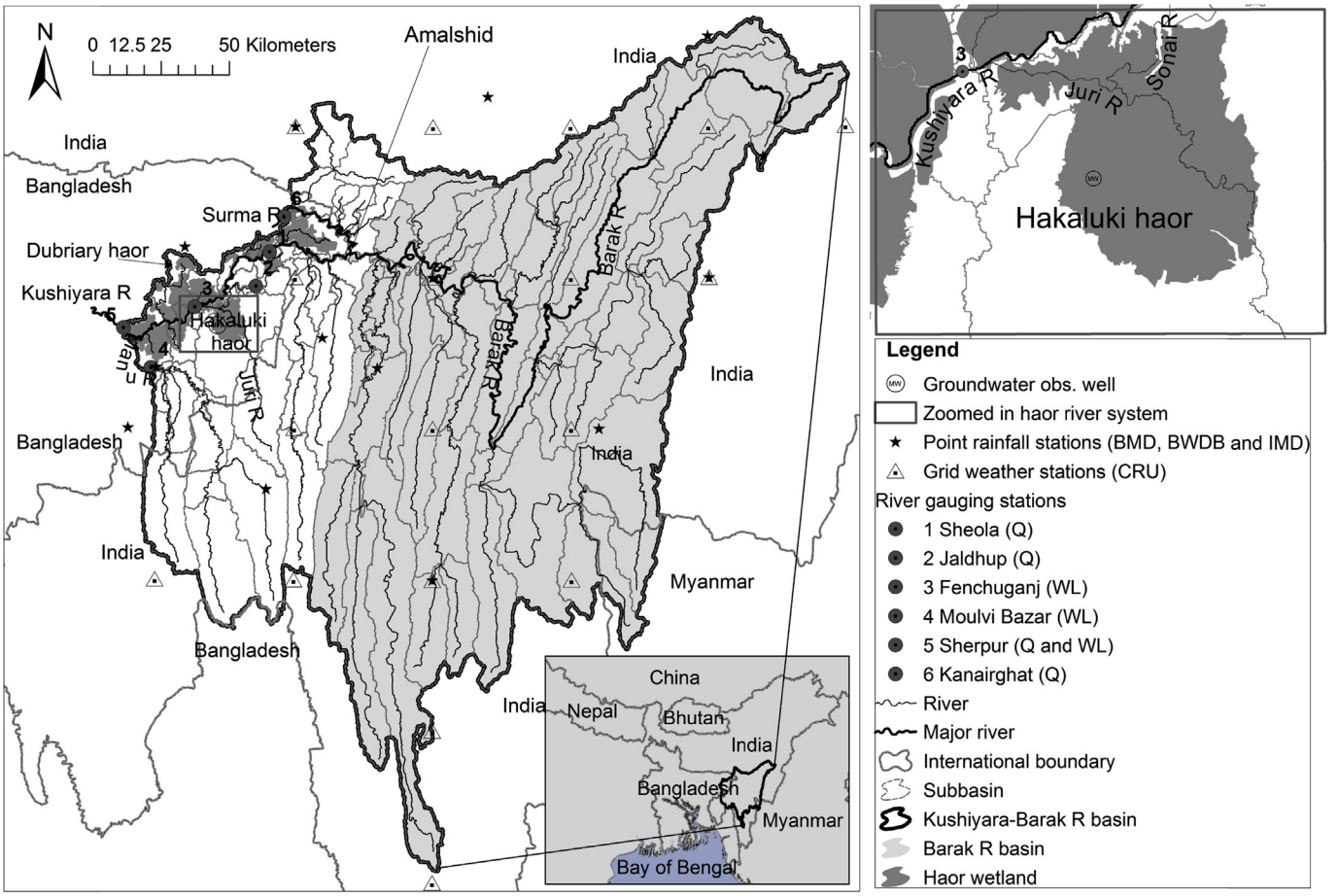

Fig. 4. The geographical location of the Barak-Kushiyara River Basin and haor wetlands. The areal extent of wetlands indicates their maximum water surface areas. Hakaluki haor is shown in the inset. Under river gauging stations, "Q" and "WL" indicate respectively discharge and water level or stage. The acronyms in the parentheses of weather station indicate data source. BMD = Bangladesh Meteorological Department, BWDB = Bangladesh Water Development, IMD = Indian Meteorological Department, CRU = Climatic Research Unit – University of East Anglia.

mass balance in both the wetland and aquifer is updated.

2.4. Study area and data collection

SWATrw was evaluated through the development of two models (the original SWAT and SWATrw) of a river basin in South Asia that is characterised by extensive riparian wetlands. The Barak-Kushiyara River Basin is named after its two main rivers, the Barak in India and the Kyshiyara in Bangladesh (Fig. 4). The basin has a total area of 35,563 km^2 of which 3,185 km^2 (9%) is within Bangladesh. With the exception of a very small fraction (<1%) in Myanmar, the remainder lies in northeastern India. Catchment elevation ranges from approximately 10 m above mean sea level (a.m.s.l.) in the extensive Bangladeshi lowlands, which are essentially flat except for a few hillocks near the Indian border, to about 3000 m a.m.s.l. in the Lushai Hills from where the Barak River originates.

Precipitation over the basin falls predominantly as rain except for hail during early monsoon storms. The hydrological year (April–March) is divided into four seasons: (i) the pre-monsoon (April–May), (ii) monsoon (June–September) during which 65% of total annual precipitation occurs, post-monsoon (October–November) and the dry season (December–March). Average annual rainfall is ~2450 mm and ranges from 1800 mm over the upper Barak River Basin to 3100 mm over the lower floodplain. Soils in the catchment vary from sandy clay loam in upper areas to loam in the lower catchment. Forest is the dominant land cover (77%) whilst the lower floodplain areas are characterised by intensive cultivated of rice.

The lower part of the basin is characterised by many riparian saucer shaped, depressional wetlands known locally as haors (CEGIS, 2012; Choudhury and Nishat, 2005; Islam, 2010). These wetlands are thought to have evolved from gradual land surface depressions; therefore, they look like saucer shaped ponds/lakes with gentle side slopes. These wetlands are traversed by or connected to the main rivers and their tributaries and so have strong interactions with the river systems. Shallow aquifers also exert an influence upon hoar hydrology. In the wet season, haors are hydraulically connected with rivers due to high water levels and are extensively inundated. During the dry season, the wetlands are isolated from the river systems as water levels fall through drainage, evaporation, and seepage. Almost all water within hoars disappears except for some deep areas, locally called beels, which are used for fish culture and irrigation. Hoar wetlands are an important agricultural resource especially for the cultivation of Boro rice, an intensively irrigated rice variety (CEGIS, 2012; Hasan and Hossain, 2013). However, pre-monsoonal flash floods generated by overbank flows frequently result in the loss of ripening Boro rice crops and as a result earth dykes have been constructed along some river channels and around some hoars. Sustainable management of hoar wetlands relies upon improved understanding of their hydrological behaviour and their influence upon catchment hydrology. This provides a major motivation for the

Table 1
Sources and characteristics of data used to build the SWAT/SWATrw models of the Barak-Kushiyara River Basin.

Data	Sources	Characteristics
Digital Elevation Model (DEM)	HydroSHEDS (**Hydro**logical data and maps based on **SH**uttle **E**levation **D**erivatives at multiple **S**cales) database (Lehner, 2005) http://hydrosheds.cr.usgs.gov/index.php	*Derived from the Shuttle Radar Topography Mission (SRTM) data *90 m horizontal resolution
Land use and land cover (LULC)	GLC (Global Land Cover) dataset http://glcf.umd.edu/data/landcover/	*Derived from AVHRR (Advanced Very High Resolution Radiometer) satellite imagery data (Hansen et al., 2000) *1 km horizontal resolution
Soil	HWSD (Harmonized World Soil Database) http://www.fao.org/soils-portal/soil-survey/soil-maps-and-databases/harmonized-world-soil-database-v12/en/	*1 km horizontal resolution *2 vertical layers: 0–300 mm and 300–1000 mm *Provides major physico-chemical properties of soils (e.g., texture, gravel, bulk density, organic matter and pH)
Rainfall	BMD (Bangladesh Meteorological Department) and BWDB (Bangladesh Water Development Board)	*Point rainfall measured at weather stations (see Fig. 4) *Temporal resolution: daily *Period: 1987–2010 *Spatial coverage: Bangladeshi part of the basin
	IMD (Indian Meteorological Department)	*District wise average rainfall *Temporal resolution: Monthly *Period: 2004–2010 *Spatial coverage: Indian part of the basin
	CRU TS 3.20 (Climatic Research Unit – University of East Anglia Time Series) climate database (Harris et al., 2014) archived in BADC (British Atmospheric Data Centre) http://badc.nerc.ac.uk/data/	*Gridded ($0.5^\circ \times 0.5^\circ$ spatial resolution) rainfall *Temporal resolution: Monthly *Period: 1987–2010 *Spatial coverage: the whole basin
Temperature	BMD	*Point data measured at BMD weather stations *Temporal resolution: daily *Period: 1987–2010 *Spatial coverage: Bangladeshi part of the basin
	CRU TS 3.20 climate database	*Gridded ($0.5^\circ \times 0.5^\circ$ spatial resolution) temperature *Temporal resolution: Monthly *Period: 1987–2010 *Spatial coverage: Indian part of the basin
Humidity, wind speed and solar radiation	CLIMWAT 2.0 database of FAO (Food and Agriculture Organization of the United Nations)	*Point data at available weather stations in the database *Temporal resolution: Long time mean monthly *Spatial coverage: the whole basin
River flow and stage	BWDB	*River flow data were generated from the previously developed rating curves *Temporal resolution: daily *Period: 1990–2010

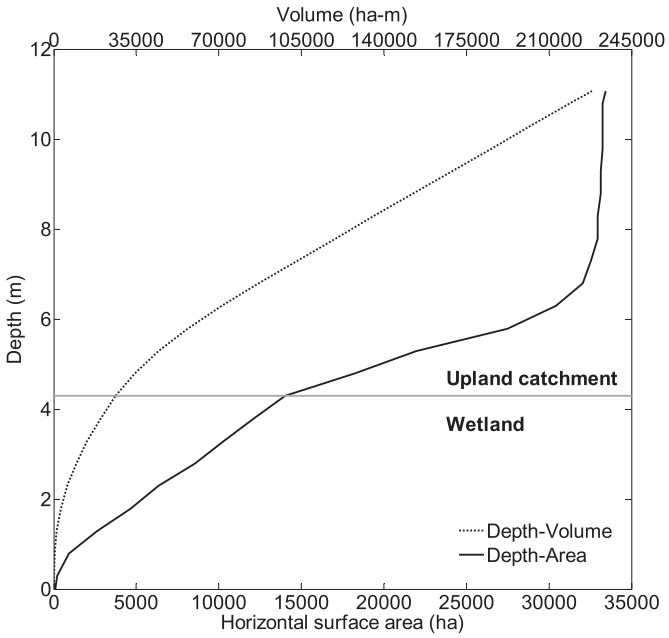

Fig. 5. The volume-area-depth relationship curves of the Hakaluki haor catchment after Choudhury and Nishat (2005).

current study.

One major hoar wetland is the Hakaluki haor that is traversed by the Juri River, a tributary of the Kushiyara River that it joins at the Fenchuganj gauging station (Fig. 4). The Sonai River is the main tributary of the Juri River. Their junction is at the north end of the Hakaluki haor. During the monsoon season, higher water stage in the Kushiyara River can cause water to flow back into the Juri River and as a result the Hakaluki haor can receive large amount of water from the Kushiyara. While data scarcity is a major hurdle for wetland research in Bangladesh's hoar region, the availability of morphometric characteristics of the Hakaluki haor, together with hydrological time series data (stream flows, river stage and groundwater level) from around the wetland, as well as elsewhere in the basin, enables the use of this particular wetland and the Barak-Kushiyara River Basin as a case study in the development of the SWATrw model.

In general the data requirements for SWAT can be grouped into four categories: a Digital Elevation Model (DEM), land use, soil and climate time series. Moreover, measured streamflow data at available gauge stations are commonly used to validate the model. Table 1 summaries the data employed within the SWAT/SWATrw models of the Barak-Kushiyara River Basin.

The study area lacks morphometric properties of wetlands except for the volume-area-depth relationship curve provided by Choudhury and Nishat (2005) for the catchment of the Hakaluki haor (Fig. 5). This morphometric curve was originally developed from the Water Development Map of 1963 (BWDB and FPCO, 1993).

For the Hakaluki haor, the area corresponding to depths of 4.29 m and lower is considered as the maximum wetland water area (13889 ha) based on the wetland areal map provided by CEGIS (2012). The required maximum wetland water surface area of other wetlands within each sub-basin was derived using the same areal map. The corresponding maximum wetland water depth was approximated based on the available documentary information (Oka et al., 2013; Uddin et al., 2012), the DEM data and Google Earth. To retrieve the required depth from Google Earth, the map (KML file) of the maximum surface area for each wetland was overlaid on Google Earth followed by manual identification of the lowest and highest elevations within each wetland. In general, the mean water depth of the haor wetlands within the basin varied from 1 m in the dry season to 6 m during the monsoon season. Once a normal elevation is determined (described in Section 2.3.2), the corresponding wetland water volume and water surface area were generated using the H-K wetland geometric model parameterised using the procedure described above. The initial water volume in each wetland was defined as the equivalent volume at 1 m depth since both the calibration and validation periods started in the dry month of January.

2.5. Simulation of the Hakaluki haor's morphometric curve

An assessment of the ability of the wetland geometric models in SWAT and SWATrw (i.e. the H-K wetland geometric model) to represent the observed morphometric characteristics of the Hakaluki haor was undertaken by simulating the wetland morphometric properties using a spreadsheet programme. First, the wetland shape parameter 'p' in the SWATrw model (see Equations (10) and (11)) was calibrated by iteratively changing its value until the simulated volume-depth and volume-area curves matched the observed counterparts as closely as possible. The observed wetland volumes were the only input variable to the calibrated model; however, this input was replaced by simulated wetland water storage in catchment-scale hydrological modelling. While calibrating 'p' the two required values of wetland area and depth at its maximum capacity were set to 13889 ha and 4.29 m, respectively. Similarly, the shape parameter (see Equation (4)) of the SWAT wetland module was calculated using two sets of known values of wetland volume and area, which were 21143 ha-m, 13889 ha and 2883 ha-m, 3841 ha, respectively at the wetland's maximum and normal water levels. All the values except the maximum wetland area (13889 ha) were obtained from the previously developed wetland volume-area-depth relationship curve by SWATrw for maximum and normal wetland water depths of 4.29 and 2.1 m. Finally, the volume-area and volume-depth curves simulated by both models were compared to the corresponding observed curves.

2.6. Model setup, calibration and validation

Models of the Barak-Kushiyara River Basin were setup using both SWAT and SWATrw. Catchment delineation was performed using the pre-defined river network, which forces SWAT to generate a more realistic network and associated sub-basins. This is particularly advantageous in low relief areas where topography is not well captured by relatively coarse DEM data. The final model had a total of 116 sub-basins that were manually inter-connected based on the river network (Fig. 4).

Each sub-basin was further discretised into HRUs using threshold values of 10, 20, and 35% for land use, soil, and slope, respectively. In general, large spatial variation of each property (land use, soil and slope) demands a smaller threshold value and thus many HRUs. Although the GLC land use classification does not contain rural villages, 5% of the rice land use area was assumed to be rural settlements since most of South Asia's rice dominated agricultural land is dotted with scattered rural villages. These villages contain homesteads, perennial trees, and road networks. Therefore, each rice land HRU was divided into two smaller HRUs; 95% of the area was classified as rice and the remaining 5% as rural village.

Since the ultimate goal of this study is to compare the simulation capabilities of SWAT and SWATrw, with a specific focus on wetland-river-aquifer interactions, the calibration and validation procedures were kept alike. Firstly the SWATrw model was calibrated, and then subsequently SWAT was run using the values of common parameters derived from SWATrw calibration. Values for four required volumetric and areal parameters (WET_VOL, WET_MXVOL, WET_NSA, WET_NVOL shown in Table 2) of SWAT were generated from the calibrated wetland morphometric curves by SWATrw using corresponding wetland water depths at maximum, normal and initial levels. The assumption behind this strategy is that wetland morphometric characteristics are well captured by the calibrated SWATrw model; therefore, a wetland property (volume or area) generated by that model for a known depth would be much better than calibrating those unknown parameters in SWAT.

The SWATrw model was manually and sequentially calibrated against observed mean monthly river discharge (2004–2010) at the Sheola, Kanairghat, Jaldhup and Sherpur gauging stations. Calibration on a monthly basis was considered appropriate since the majority of daily climate data were stochastically derived from monthly values (see Thompson et al., 2013). In addition, the daily time series of observed river discharge was characterised by periods of missing data. The simulated river water depth was found to be very sensitive to the CH_N2 parameter (Manning's roughness coefficient for a river). Therefore, the value of CH_N2 calibrated against monthly discharge was further fine-tuned using daily river stage data from the Fenchuganj, Moulvi Bazar and Sherpur gauging stations that had comparatively fewer gaps in their records. Once a satisfactory result was attained, the consistency of model performance was validated using the period 1990–2003.

In addition to graphical comparisons of observed and simulated river discharge, model performance was statistically evaluated using commonly used metrics: Nash-Sutcliffe efficiency (NSE) (Nash and Sutcliffe, 1970), percent bias (PBIAS) (ASCE, 1993; Moriasi et al., 2007), ratio of root mean square error to the standard deviation of observed data (RSR) (Moriasi et al., 2007), and the coefficient of determination (R^2) (also see Moriasi et al., 2007). Moriasi et al. (2007) reviewed a number of model performance metrics and their application in a wide range of catchments. They concluded that a catchment model can be sufficiently evaluated by using the combined values of the first three statistical metrics (NSE, PBIAS and RSR) and presented a generalised framework for such an evaluation.

A sensitivity analysis with the TEDPAS (Temporal dynamics of parameter sensitivity) method (Reusser et al., 2011) was conducted to investigate how the newly incorporated wetland parameters influence on streamflows and wetland water storages (or water balance). TEDPAS estimates sensitivity of each parameter at each time step based on the FAST (Fourier Amplitude Sensitivity Test) global sensitivity analysis approach (Cukier et al., 1975, 1973). Time series of parameter sensitivities generated by TEDPAS during a simulation period help to identify dominant hydrological processes and their duration of existence (Guse et al., 2014; Reusser and Zehe, 2011). The sensitivity for a particular parameter at a time step is estimated based on the first-order partial variance approach (Reusser et al., 2011). In this study TEDPAS was employed using the calibration period for the two sub-basins respectively containing Hakaluki haor and Dubriary haor (a

Table 2
Calibrated parameters governing hydrological processes*.

Models	Parameters	Description (unit)	Default values	Calibrated values
SWAT & SWATrw	Basin level			
	SURLAG[a]	Surface runoff lag coefficient (day)	4.00	0.10
	HRU level			
	CN2[a]	Curve number	70–92	60–81
	ESCO[a]	Soil evaporation compensation factor	0.95	0.25–0.95
	EPCO[a]	Plant uptake compensation factor	1.00	0.30–1.00
	GW_DELAY[a]	Groundwater delay (day)	31	10–45
	ALPHA_BF[a]	Baseflow factor (day)	0.048	0.01–0.048
	SHALLST	Initial depth of water in shallow aquifer (mm)	0.50	1.00–1300.00
	GWQMN	Threshold depth of water in shallow aquifer for baseflow (mm)	0.00	0.00–1280.00
	REVAPMN	Threshold depth of water in shallow aquifer for revap (mm)	1.00	0.00–2000.00
	RCHRG_DP[a]	Fraction of soil percolated water to deep aquifer	0.05	0.05–0.80
	GW_SPYLD	Specific yield of shallow aquifer	0.003	0.003–0.02
	Sub-basin level			
	CH_N2	Manning's roughness coefficient for a river	0.014	0.013–0.017
	WET_FR	Fraction of sub-basin area drained into a wetland	–	0.82–1.00
	WET_MXSA[b]	Maximum wetland water surface area (ha)	–	372–14869
	WETEVCOEF[a]	Wetland evaporation coefficient	–	0.40–0.60
	WET_K[a]	Hydraulic conductivity of wetland bottom (mm/hr)	–	0.30–8.00
SWAT	WET_VOL	Initial volume of water in wetlands (ha-m)	–	22–894
	WET_MXVOL	Maximum wetland water volume (ha-m)	–	419–29748
	WET_NSA	Normal wetland water surface area (ha)	–	108–11764
	WET_NVOL	Normal wetland water volume (ha-m)	–	58–22264
SWATrw	WET_D	Initial wetland water depth (m)	–	1.00
	WET_DMX[b]	Maximum wetland water depth (m)	–	3.00–8.00
	WET_P[a]	Wetland shape factor	–	1.1–1.5
	WET_TH[b]	Thickness of wetland bottom (m)	–	1.00
	CCH_M[b]	Depth exponent in connecting channel flow equation	–	2.00
	CCH_N[b]	Slope exponent in connecting channel flow equation	–	1.00
	CCH_SF[b]	Friction slope of connecting channel	–	0.01
	CCH_DFR[a]	Fraction of main channel maximum depth at normal level	–	0.10–0.80
	CCH_LFR[a]	Fraction of main channel length to be overflowed at normal level	–	0.10–0.90
	CCH_C	Conveyance coefficient of connecting channel (m^{-1} s^{-1})	–	667.00

*Parameters are grouped based on models (SWAT and SWATrw) and spatial scales (basin, sub-basin and HRU). Parameters within "SWAT & SWATrw" mean both the models use these parameters. Basin level parameter indicates that all HRUs in the basin use the same value of that parameter. Under sub-basin level, the value of each volumetric, areal and CCH_LFR wetland parameters is apportioned among HRUs according to their respective areal extents in the sub-basin; values of other sub-basin level parameters are unique for all HRUs in the sub-basin.

[a] These parameters are used for sensitivity analysis (see Section 2.6).

[b] These parameters were not calibrated rather their values were taken from available data, literature and in some cases approximated based on the author's detailed knowledge of the study area.

Table 3
Parameter range for sensitivity analysis.

Parameters[a]	Range of parameter value	
	Hakaluki haor sub-basin	Dubriary haor sub-basin
SURLAG	0.05–1.0	0.05–1.0
CN2	55–85	65–80
ESCO	0.3–1.0	0.3–1.0
EPCO	0.3–1.0	0.3–1.0
GW_DELAY	5–40	5–31
ALPHA_BF	0.1–1.0	0.01–1.0
RCHRG_DP	0.0–0.8	0.0–0.8
CCH_DFR	0.1–0.8	0.1–0.8
CCH_LFR	0.1–1.0	0.1–1.0
WET_P	0.5–2.0	0.5–2.0
WET_K	0.1–2.0	1.0–10
WETEVCOEF	0.4–0.8	0.4–0.8

[a] Their names are explained in Table 2.

similar sized wetland, Fig. 4). Unlike conventional practices where sensitivity analysis precedes model calibration, we followed the reverse practice. Our intention is not to identify sensitive model parameters but to rather see how the parameters of an already carefully manually calibrated model influence target hydrological components (streamflows and wetland water balance). Accordingly parameter ranges were chosen around the corresponding calibrated parameter value (Table 3). Table 4 summaries the major distinguishing characteristics of the two sub-basins related to modelling their wetlands. Streamflows of the sub-basin containing the Hakaluki haor are influenced by its river flows generated by upstream sub-basins whereas this is not the case for the second sub-basin in which Dubriary haor is located. For the 12 parameters (see Table 2) that are thought to have a major influence on streamflows and wetland water balance, TEDPAS produced 579 parameter sets (i.e. 579 model runs at each time step of the simulation period).

3. Results and discussion

3.1. Simulated morphometric properties of the Hakaluki haor wetland

The calibrated values of the two paired morphometric parameters (shape and scale) are 0.65 and 22.54 for SWAT and 1.1 and 983 for SWATrw. Fig. 6 shows the volume-area and volume-depth relationships from both models and those derived from the observed morphometric data for the Hakaluki haor. Both the models produce identical volume-area curves (Fig. 6a) that closely match ($R^2 = 0.99$ and slope of the observed vs simulated line = 1.1) the observed until the wetland volume reaches 14200 ha-m. Subsequently for a given volume the wetland areas are consistently overestimated so that the existing models are unable to represent the natural morphometric properties of the Hakaluki haor catchment. This is because the geometry of the upland catchment differs markedly

Table 4
Major distinguishing characteristics of the two sub-basins containing Hakaluki and Dubriary haor wetlands.

Characteristics	Sub-basin containing the Hakaluki haor wetland	Sub-basin containing the Dubriary haor wetland
Area of sub-basin (ha)	79200	24200
Streamflows influenced by inflows from upstream sub-basins	Yes	No
Wetland drainage area (ha)	78408 ha (99% of the sub-basin)	23232 ha (96% of the sub-basin)
Maximum wetland water surface area (ha)	13889 (18% of the sub-basin)	13882 (57% of the sub-basin)
Maximum wetland water depth (m)	4.29	5.00
Hydraulic conductivity of wetland bottom (mm/hr)	0.1	1.0
Maximum main channel depth (m)	2.42	1.17

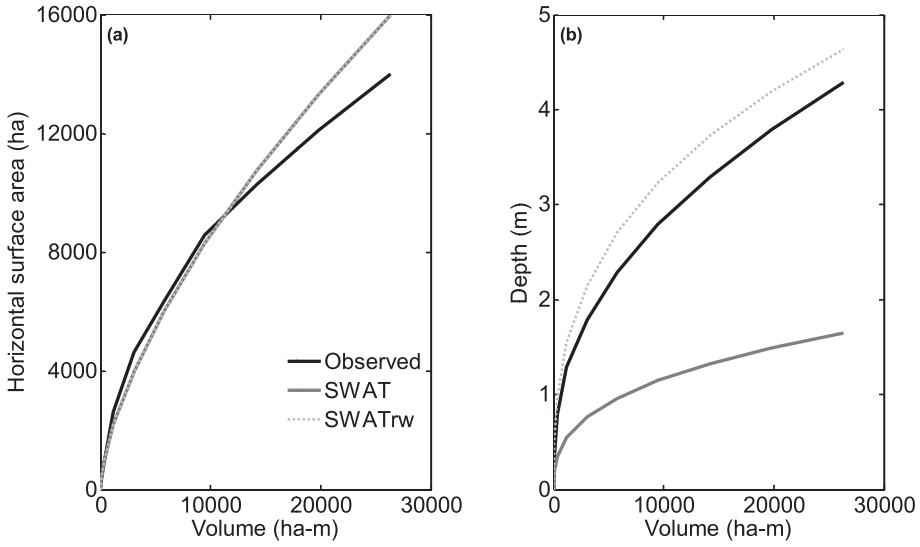

Fig. 6. Comparison of wetland morphometric properties simulated by SWAT and SWATrw for the Hakaluki haor wetland.

from that of wetland (Fig. 5). While exploring the reason for the two models' identical volume-area curves, it was found that the values of the wetland's shape and scale factors become the same if SWATrw's wetland formulas (Equations (10) and (11)) are rearranged to the form of SWAT's wetland volume-area relationship (Equation (3)). This is intuitively because the wetland volumes and areas at maximum and normal levels required by SWAT originated from the SWATrw generated wetland morphometric curve (see Section 2.5). This argument was further confirmed for other wetlands in the basin (not shown).

Unlike the volume-area relationship, the volume-depth relationships from the two different models vary markedly and exhibit different abilities in emulating the observed relationship for the Hakaluki haor (Fig. 6b). The relationship for the SWATrw model provides a good approximation to the observed (R^2 = 0.99 and slope of the observed vs simulated line = 1.1). Depths are slightly overestimated by on average 15% across the full range of volumes. On the other hand, SWAT consistently underestimates (R^2 = 0.99 and slope of the observed vs simulated line = 0.38) the actual wetland depths by on average 58%. Since for a given volume both models simulate exactly the same surface area, a shallower wetland simulated by SWAT for that volume must be more cylindrical (i.e. higher side slope) than that of SWATrw. As discussed in Section 2.3.1, Equation (9), which was proposed by Liu et al. (2008) for SWAT, assumes an equal side slope of 1/4 for both a riparian wetland and an associated floodplain. The DEM data suggest that the average side slope of the Hakaluki haor wetland is 2%, much smaller than SWAT's representation of the wetland (25%). The large differences in the wetland morphometric relationships, and the considerable underestimation of depth by SWAT, demonstrate the potential difficulties in applying SWAT where depth-dependent hydraulic simulations of wetland interactions with rivers and aquifers are required.

3.2. Calibrated parameters and simulation performance

A total of 30 parameters were selected for calibration (Table 2). Of these, the first 16 in Table 2 are common to both the models. The next four are limited to SWAT and the last 10 to SWATrw. A precise interpretation of calibrated parameters within a conceptual model is not possible because different combinations of values of the same parameters may produce an almost identical simulation as explained by the equifinality concept (Beven and Freer, 2001). However, the relative influence of 12 selected parameters (Table 2) on hydrological processes, derived from TEDPAS analysis, is discussed below. The value of the only basin level calibrated parameter, SURLAG, was found to be 0.1. This relatively low value compared to the default 4.0 indicates that surface runoff generated within a sub-basin moves at a moderate rate towards its river system. A catchment with flat topography and/or higher resistance to overland flow generally responds relatively slowly at the outlet to the generated overland flow. Although the lag time of surface runoff for steep sloped headwater catchments would be expected to be smaller, the lower flat topographic properties of the extensive lowland parts of the basin leads to the smaller value of SURLAG. Stream flows at all gauging stations that are in the lower floodplains of the basin are predominantly characterised by the floodplain flow dynamics. For example, a steep hydrograph produced at the foothill of an upper sub-basin is likely to be diffused in the lower floodplain.

The curve number for the moderate antecedent moisture

condition (CN2) plays a major role in separating rainfall that reaches the ground into infiltrated water and surface runoff. Table 2 shows the initial values because the model automatically updates CN2 based on simulated daily soil moisture. The soil evaporation compensation factor (ESCO) enables the model to meet evapotranspiration demands from the deeper soil layer if necessary. The calibrated values of ESCO varied between 0.25 for forested hilly HRUs to the default value of 0.95 for rice dominated floodplain HRUs that are characterised by much wetter soils. Another calibrated soil or unsaturated zone parameter is the plant uptake compensation factor (EPCO) which controls how much of the plant water demand (transpiration) that is not satisfied by the upper soil layer is drawn from the underlying soil layer. The calibrated values of EPCO for HRUs dominated by forest and tea land covers were higher (0.6–1.0) compared to rice dominated HRUs (a consistent 0.3). An explanation could be associated with the soil profile and plant root properties. For the entire basin, a 2-layered 1000 mm soil profile was used with the top and bottom layers having specified depths of 300 mm and 700 mm, respectively. A reasonable assumption is that the root depths of mature forest trees and tea shrubs will extend below the depth of the top layer, which allows plants to satisfy their water demand from the lower soil layer. However, the root depth of rice generally varies between 0 and 300 mm (Sharma et al., 1994; Uddin et al., 2009) so that the contribution of water from the deeper soil layer to transpiration is negligible unless water stress occurs. In any one year, the simulated rice experienced water stress for no more than 15% of the total growing period suggesting that transpiration from deeper layers was limited.

Seven calibration parameters (GW_DELAY to GW_SPYLD in Table 2) are associated with the groundwater simulation. Although SWAT does not directly use any observed data beyond the soil profile, a prior knowledge of the aquifer properties within a river basin may assist the calibration process by appropriately parameterizing the groundwater model. For the Bangladesh part of the basin, calibrated values of SHALLST, GWQMN and GW_SPYLD were 1300 mm H_2O, 1280 mm H_2O and 0.02, respectively. Calibration of these parameters benefitted from data provided by Shamsudduha (2010) who produced spatial geological properties of the local aquifers compiled from multi-source field data. These calibrated values yield an initial GWL of 1 m ((1300−1280)/(0.02*1000)) above the riverbed level. Such a low GWL eventually produces negligible base flow in the dry season (MPO, 1991; WARPO, 2000; cited in Shamsudduha, 2010). Since the simulation period starts on the first day of January 1990 (validation) or 2004 (calibration), these calibrated parameters can be considered reasonable for the Bangladesh part of the basin. In the absence of sufficient field data, it is not possible to further explore and justify the calibrated values of the other groundwater parameters.

All of the sub-basin level calibration parameters are associated with wetland simulation except CH_N2 for river simulation. The range of values of each parameter shown in Table 2 is based on the results of all the wetlands or rivers in the basin. Most of the rivers in the upper hilly region employed the default value (0.014) for CH_N2 whilst lower floodplain rivers had slightly higher values (0.015–0.017). More resistance to flow from instream vegetation could account for the larger CH_N2 for the river system in the lower floodplain. The parameter WET_MXSA was not directly calibrated but instead its values were obtained from the CEGIS wetland shape file.

The high calibrated values of WET_FR (0.82–1.00) replicate the reality of the basin's floodplains where a large proportion of local surface runoff flows towards wetlands rather than rivers. The two most important SWATrw parameters are CCH_DFR and CCH_LFR because they exert the largest influence upon the quantity of transferable water during wetland-river interaction through the connecting channel. In general, a combination of deeper river reaches and a greater distance between river and wetland results in larger values of CCH_DFR and smaller CCH_LFR values whereas the opposite combination (a shallower river reach and a shorter distance between river and wetland) produces the opposite results. For all connecting channels, the value of the calibrated conveyance coefficient (CCH_C) was found to be 667 m^{-1} s^{-1}. Kadlec and Wallace (2009) suggested values for densely or sparsely vegetated wetlands of 116 and 580 m^{-1} s^{-1}, respectively. The higher CCH_C value for the connecting channels within the SWATrw model indicate relatively low resistance which reflects the channelized nature of the river-wetland exchanges in which water is relatively deep in comparison to overland flow across a wetland's surface.

Fig. 7 shows the temporal sensitivity of different parameters to streamflows, wetland water volumes and wetland water surface areas simulated by SWATrw for the sub-basin containing Hakaluki haor (Fig. 4). The surface runoff parameter SURLAG and groundwater parameter RCHRG_DP show greater sensitivity (as large as 0.8) to streamflows during the three rainy periods (pre-monsoon, monsoon and post-monsoon) compared to the other parameters (Fig. 7a). However, sensitivity of SURLAG to streamflows is comparatively higher and occurs earlier than that of RCHRG_DP. The other surface runoff parameter CN2 is found sensitive during the pre-monsoon season (April and May) when separate storms separated by dry spells cause soils to be alternatively wetted and dried. However, its influence on streamflows gradually dampens in the subsequent monsoon (June–September) and post-monsoon (October–November) seasons when consistently wetter soil prevails. SWATrw/SWAT updates the value of CN2 depending on soil water content in each time step. In the wet season soil remains almost saturated leading less variable CN2 and thus a smaller sensitivity to streamflows. The sensitivity of the soil evaporation parameter ESCO at the beginning of the wet season demonstrates the influence of soil water content on streamflows at this time. The two groundwater parameters related to lag time, GW_DELAY and ALPHA_BF, become dominant over other parameters during the early dry season (December and January). Surprisingly a very small sensitivity value (0–0.02) for each of the wetland parameters (WETEVCOEF, WET_K, WET_P, CCH_LFR and CCH_DFR) indicates that the presence of the wetland has little influences on streamflows from the Hakaluki haor sub-basin. These results demonstrate that streamflow in this sub-basin during the three wet seasons of the simulation period is mainly influenced by overland routed surface runoff, and then secondly by baseflow. Wetland routed runoff (i.e. surficial exchange between the wetland and river) has a relatively small influence. Since CN2 remains relatively less sensitive during the period of almost continuous monsoonal rainfall, modelled surface runoff can be categorized as a non-Hortonian process driven by soil saturation. In contrast to GW_DELAY and ALPHA_BF, the larger sensitivity of RCHRG_DP during the monsoon indicates that the availability of water from the shallow aquifer is the prime determinant of baseflow rather than the aquifer's transmitting properties. This relative influence of aquifer storativity and transmissivity on streamflows reverses during the dry period as groundwater levels decline. Since baseflow can only occur if the available water in a shallow aquifer is greater than a specified threshold value (i.e. GWQMN), the noticeable sensitivity of ALPHA_BF (0.1–0.35) on wetland water volume (Fig. 7b) indicates a considerable influence of wetland shape factor (WET_P, sensitivity = 0.2–0.5) on baseflow during late May – mid October. This happens through wetland-groundwater interactions controlled by parameters WET_K and WET_P in addition to driving hydraulic head potentials. In dry periods, wetland water balance can be almost completely explained by WET_P. This suggests the

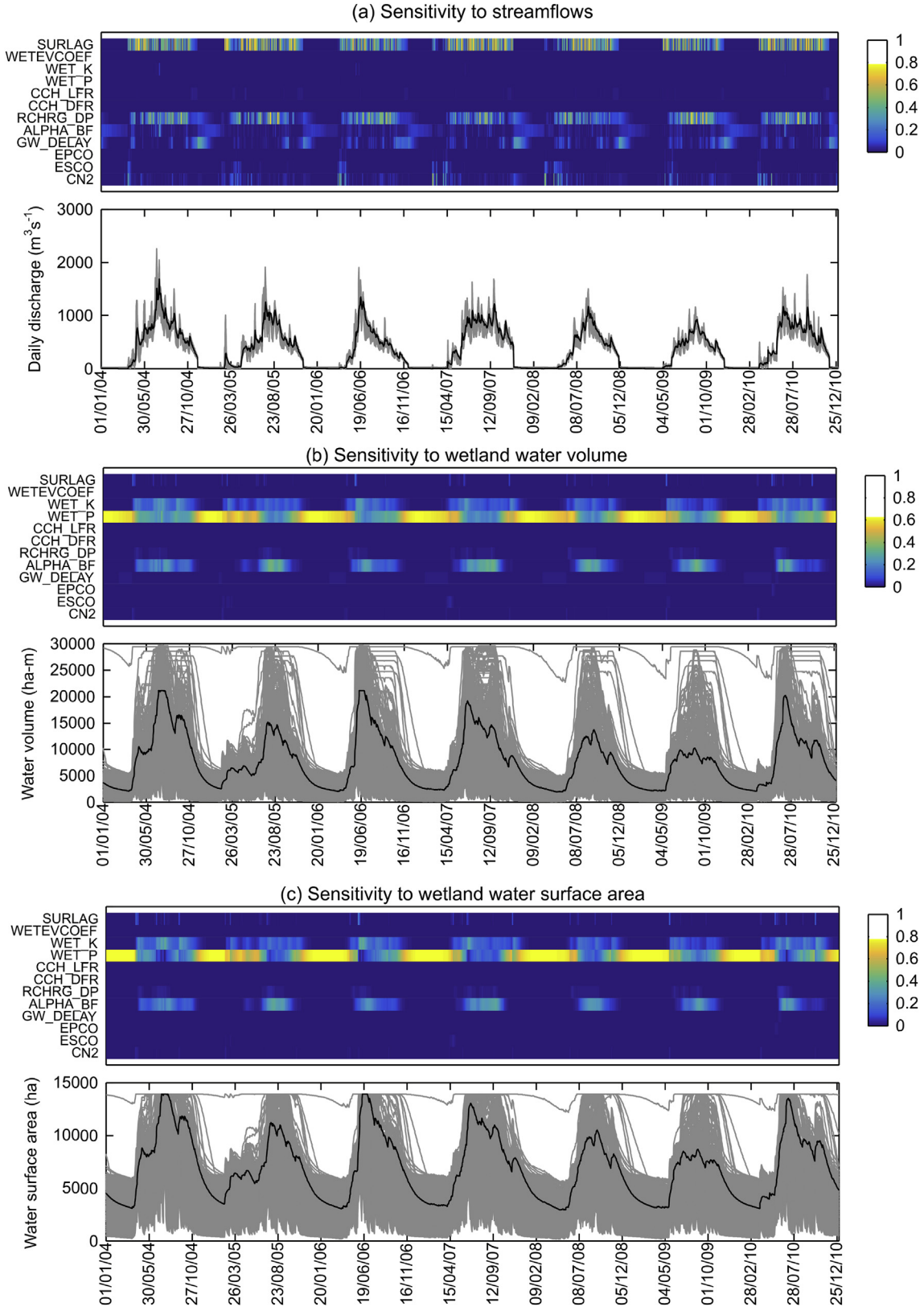

Fig. 7. Temporal parameter sensitivity to (a) streamflows, (b) wetland water volume and (c) wetland water surface area for the Hakaluki haor sub-basin. All parameters are described in Table 2. The colour ramp represents sensitivity of the parameters. The line plots indicate time series of target simulated variables (streamflows, wetland water volume and surface area) for all 579 simulations during TEDPAS analysis. The back line is for the calibrated parameter set.

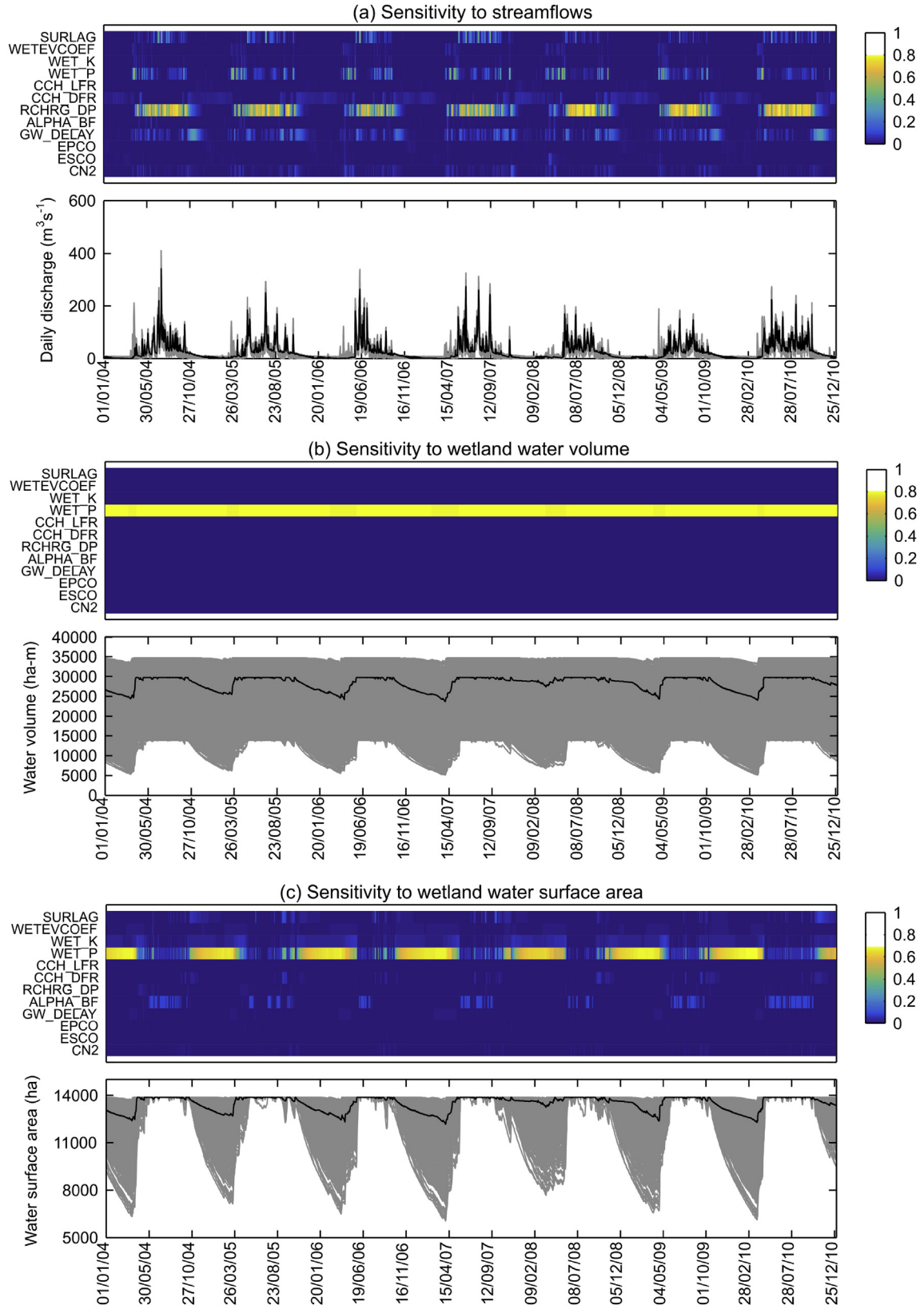

Fig. 8. Temporal parameter sensitivity to (a) streamflows, (b) wetland water volume and (c) wetland water surface area for the Dubriary haor sub-basin (description of figure components as Fig. 7).

existence of less active hydrological processes (interactions between wetland-river-aquifer, evaporation) compared to the wet season. Since wetland water surface area and depth are a direct function of wetland water volume (see Equations (10) and (11)), a

similar explanation for these two former wetland variables can be expected (Fig. 7c).

As discussed previously, it was not possible to investigate how wetland-river interaction affects the streamflow from the Hakaluki haor sub-basin because flows were found to be insensitive for the newly incorporated wetland parameters (WET_P, CCH_LFR and CCH_DFR). A probable reason for this is that the streamflows of the Hakaluki haor sub-basin are strongly influenced by inflows from upstream sub-basins that do not contain any wetlands (Fig. 4). These inflows mask any wetland related influences upon the flows at the downstream end of Hakaluki haor sub-basin.

Wetland-river interactions can, however, be investigated using the sensitivity results for the Dubriary haor sub-basin (Fig. 8) where flows are not affected by any upstream inflows and in which wetland water occupies a relatively large fraction of the sub-basin area (57%, see Table 4). Large sensitivity for WET_P and a contrasting weak influence of SURLAG (Fig. 8a) demonstrate the wetland's influence on streamflows. Moreover, the ranges of SURLAG and WET_P were identical for both the sub-basins (Table 3), therefore the sensitivity dissimilarity between sub-basins cannot be linked to the different space of each individual parameter. Rather such dissimilarity may arise from the differed hydrological behaviours between the two sub-basins. Since WET_K shows less sensitivity (0–0.05) to streamflows (i.e. groundwater is not greatly affected by wetland seepage), a strong wetland-river interaction is evident. This argument can be partially verified with the sensitivity signals of CCH_DFR (0.05–0.15) that defines the connecting channel bed elevation (or normal level). Sensitivity to CCH_DFR mainly appears during the post-monsoon period (October–November) until the next early pre-monsoon (April). It disappears during the monsoon season. This suggests that wetland-river interaction occurs via the connecting channel during the rising and falling periods of wetland water level and then via direct transfer of water beyond the wetland maximum level in the monsoon (Fig. 8c). As discussed in Section 2.3.2, this transferred water may subsequently inundate the river floodplain depending on the river's maximum capacity. Although in both SWAT and SWATrw water on a floodplain can seep to the underlying aquifer through the entire floodplain area, the reverse process is restricted. Instead seepage water can return to river through baseflow that is not a function of the area through which it flows. Recently Sun et al. (2015) addressed this issue by employing Darcy's equation in catena based discretised floodplain land units. As in the Hakaluki haor sub-basin, baseflow that is scaled by the sensitivity of groundwater parameters (RCHRG_DP, ALPHA_BF and GW_DELAY) is the larger contributor to streamflow compared to surface runoff. This baseflow is plausibly the direct response to large aquifer recharge through the sub-basin's highly conductive upland soils (hydraulic conductivity = 4–8 mm/h). A constant sensitivity signal of ~0.8 (yellow) for WET_P throughout the simulation period shows that the variance in wetland water volume is completely explained by the geometry of wetland (Fig. 8b). Hydrological processes involving the remaining 11 parameters (sensitivity ~0) have no influence on wetland water balance. Although this result is in agreement with the Hakaluki haor sub-basin for the dry period it differs for the wet period. From Fig. 8c, the water surface area of the Dubriary haor wetland remains almost static for all model runs (i.e. all parameter sets) at its maximum level (area = 13882 ha; depth = 5 m) during wet periods. However, this is not the case for wetland water volumes (Fig. 8b) since the wetland's capacity varies with its shape factor (WET_P) despite constant surface area and depth at the maximum water level. Because all vertical hydrological processes (e.g. precipitation, evaporation, wetland-aquifer interaction) in the modelled wetland occur through its water surface area, the invariance of this area among model runs at a particular time step suggests a stable state for all of these processes. For this reason variance in simulated wetland water volumes caused by the associated process-based parameters is not seen in the wet periods. Nonetheless, one might expect some variation due to groundwater parameters because (i) wetland-aquifer interaction is not only affected by water surface area but also hydraulic head differences and hydraulic conductivity and (ii) streamflow is sensitive to groundwater parameters. For most of the time wetland water level remains very close to both the ground surface and GWL whilst the range of wetland hydraulic conductivity is very small (0.1–0.3 mm/h). Therefore, only small water transfer rates between the wetland and aquifer are likely and they have extremely small impacts on the water volume of the comparatively large wetland water volume. GWL and the wetland water level are close to the ground surface in the Dubriary haor sub-basin due to its particular physiographic settings. The river bed is much closer to the ground surface than in the Hakaluki haor sub-basin (see Table 4). Because baseflow to the river cannot cause the GWL to fall beyond the river bed, GWL can only fluctuate above the river bed unless water is lost from the aquifer by other means (e.g. aquifer exchange to the wetland). Again a wetland can only intercept aquifer water when the wetland water level is below GWL. This did not happen for the Dubriary haor wetland, at least during wet periods, because wetland water level was always at maximum capacity (i.e. the ground surface level). The above interpretation of hydrological processes, involved in the two sub-basins, with respect to temporal parameter sensitivity is thought to be plausible as previously TEDPAS was evaluated for such credibility (Pfannerstill et al., 2015).

The performance of the two models is demonstrated graphically in Fig. 9 and Fig. 10. The first of these figures shows observed and simulated mean monthly discharge at four gauging stations for the calibration and validation periods. Observed and simulated daily mean stage at three stations for the same period is shown in Fig. 10. Model performance statistics for both sets of comparisons are summarised in Table 5. The performances at the two upper gauging stations (Sheola on the Kushiyara River and Kanairghat on the Surma River) are first investigated since the discharges at these locations are principally controlled by runoff from the upper Barak River Basin (see Fig. 4). The influences of floodplain wetlands on river discharge at these locations are limited and so SWAT and SWATrw can be expected to provide similar results. This is demonstrated in the very similar, and in some cases, identical model performance statistics for the two models (Table 5). For the calibration period the values of these statistics fall in the top “very good” category suggested by Moriasi et al. (2007). An annual water balance study of the Barak River shows that, for both models, 574 mm of water is on average lost as actual evapotranspiration during the calibration period. This is equivalent to 23% of annual average rainfall (2443 mm). Jhajharia et al. (2012) found that potential evapotranspiration (PET) demands over this part of the basin are about 1100 mm year^{-1} and that the highest monthly PET of 110–150 mm is in May. These values are very close to those employed in both hydrological models (1115 and 121 mm, respectively). Model results suggest that both SWAT and SWATrw are able to simulate the hydrological dynamics of the hill and forests dominated upper Barak River Basin.

Similarly, both SWAT and SWATrw show nearly equally satisfactory river discharge simulation results for the Jaldhup and Sherpur gauging stations during the calibration period. It is evident, however, that SWATrw does underperform compared to SWAT at the latter station that is located at the basin's outlet. Fig. 9d shows that peak flows at Sherpur simulated by SWATrw are slightly higher (~2%) than those of the SWAT model and this accounts for the weaker PBIAS value in Table 5. However, it is clear that SWATrw outperforms SWAT in simulating daily river stage at Fenchuganj

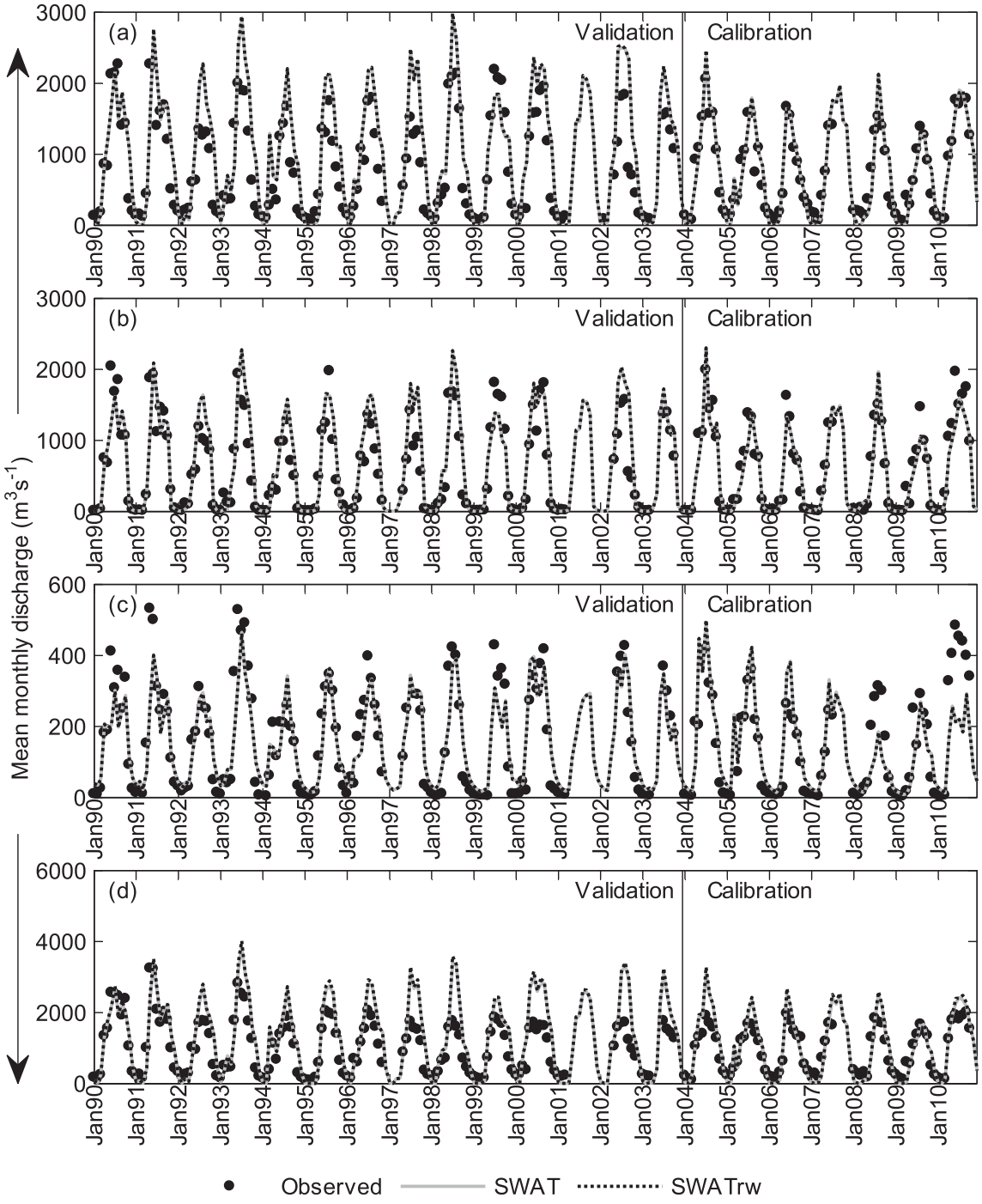

Fig. 9. Graphical representation of SWAT and SWATrw performance in simulating mean monthly river discharges at four stations Sheola (a), Kanairghat (b), Jaldhup (c), and Sherpur (d).

(Fig. 10a) and Sherpur (Fig. 10c). These two gauging stations are downstream of many wetland areas suggesting that the different performance of the two models is related to the alternative approaches used to represent wetlands within the two models. In contrast, identical simulation performance of the two models in terms of daily river levels at Moulvi Bazar (Fig. 10b) is indicated by the performance metrics (Table 5). This gauging station is downstream of a series of sub-basins that do not contain any wetlands (see Fig. 4) and so both models respond identically.

An interesting disparity between the models is evident when their simulated discharge and river stage results for the Sherpur gauging station are analysed simultaneously. Although SWATrw-generated peak flows are higher than those produced by SWAT (Fig. 9d), the former model simulates lower river stages (Fig. 10c). This is reflected in the reduced PBIAS values in both the calibration (0.17%) and validation (−12.26%) periods (Table 5). The higher outflows at Sherpur for SWATrw are associated with the larger inflows from the upstream river. This is intuitively because all upstream wetlands collectively produce more inflows at the inlet of the Sherpur river reach (the portion of Kyshiyara River that lies in the lowest sub-basin) compared to SWAT. Larger inflows to the river system simulated by SWATrw should have produced higher

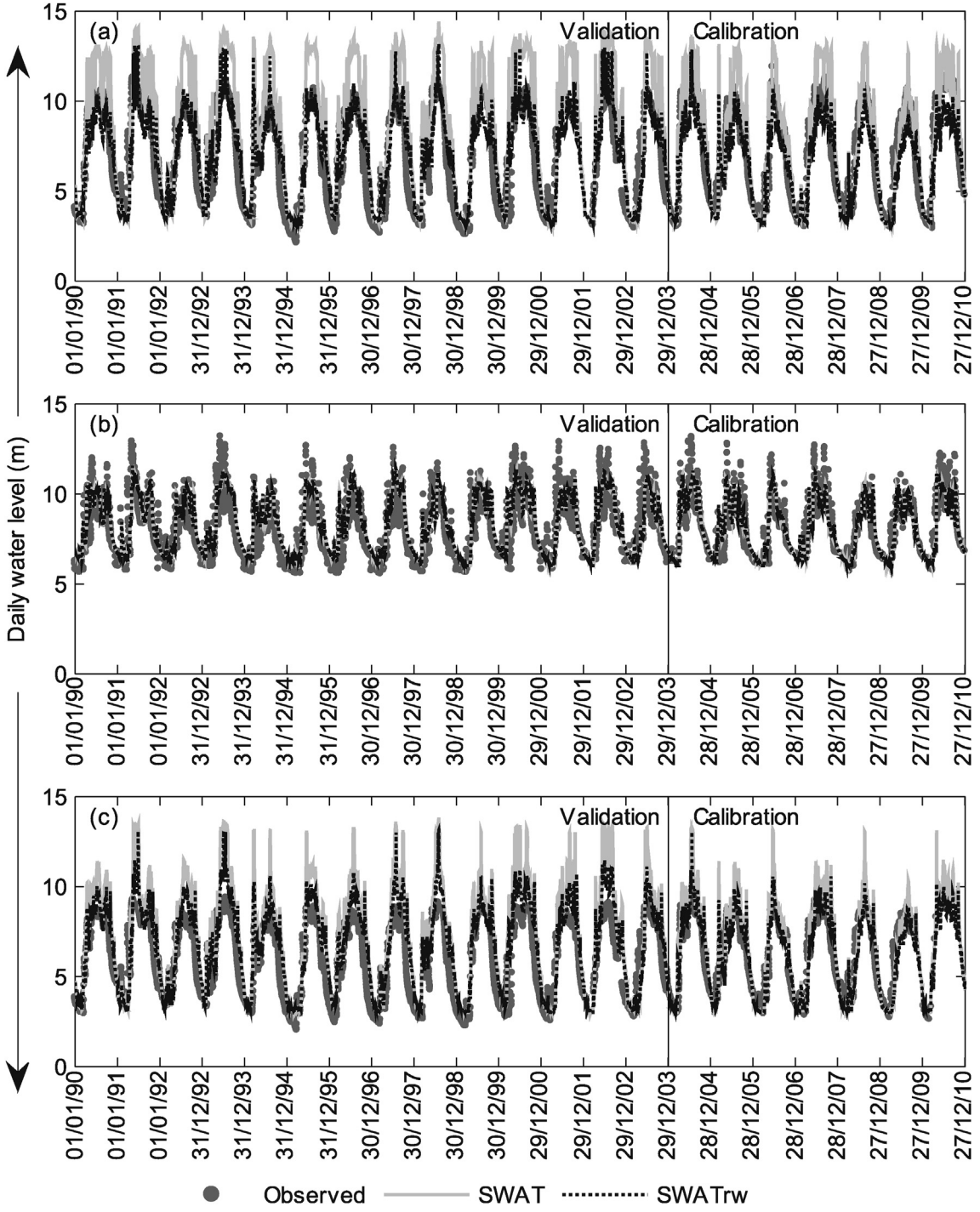

Fig. 10. Graphical representation of SWAT and SWATrw performance in simulating daily river stages/water levels at three stations Fenchuganj (a), Moulvi Bazar (b) and Sherpur (c).

river stages than SWAT; however, this was not seen in the Sherpur river reach. While routing flows through a river reach, inflows to its inlet are the sum of outflows from its upstream river(s), water yield from the associated sub-basin and initial (beginning of each time step) stored water in the river reach. The volume of this total inflow is used to estimate the water depth in a river reach based on the Manning's formula. Therefore, any changes in this total inflow will affect river water depths and downstream flows. An investigation of wetland-river interaction in the sub-basin associated with the Sherpur station reveals that the SWATrw model transfers a daily flow of 5–40 $m^3 s^{-1}$ from the Sherpur River reach to the connected wetland throughout the wet seasons (pre-monsoon, monsoon and post-monsoon). This reduction in total inflows to the reach compared to SWAT produces smaller river water depths, thus lower river stages. However, this reduction in total inflows has negligible effects on routed downstream outflows from the reach. The reasons are twofold: (i) the amount of daily water transferred from the river to the wetland is small (5–40 $m^3 s^{-1}$) compared to the increased daily river inflows (50–800 $m^3 s^{-1}$) from upstream rivers and (ii) while routing inflows to the downstream outlet, storage within the

Table 5
Statistical performance metrics for simulated monthly stream flows and daily river stages/water levels during calibration (2004–2010) and validation (1990–2003) periods.

Variables	Gauging stations	Period	Values of performance metrics							
			NSE		RSR		PBIAS		R^2	
			SWAT	SWATrw	SWAT	SWATrw	SWAT	SWATrw	SWAT	SWATrw
Mean monthly river flow ($m^3 s^{-1}$)	Sheola	Calibration	0.87	0.87	0.36	0.36	−1.66	−2.24	0.90	0.90
		Validation	0.54	0.52	0.68	0.69	−30.45	−31.78	0.78	0.78
	Kanairghat	Calibration	0.89	0.89	0.32	0.32	7.00	7.31	0.90	0.90
		Validation	0.77	0.76	0.48	0.49	−15.47	−15.71	0.83	0.83
	Jaldhup	Calibration	0.62	0.62	0.62	0.62	6.88	7.34	0.63	0.62
		Validation	0.81	0.81	0.43	0.43	2.24	2.94	0.83	0.83
	Sherpur	Calibration	0.69	0.64	0.55	0.60	−9.67	−12.30	0.80	0.90
		Validation	0.36	0.28	0.80	0.85	−32.93	−35.47	0.80	0.80
Daily river stage (m)	Fenchuganj	Calibration	0.71	0.80	0.54	0.45	−9.95	7.56	0.85	0.85
		Validation	0.31	0.79	0.83	0.45	−23.65	−2.67	0.82	0.80
	Moulvi Bazar	Calibration	0.73	0.73	0.52	0.52	−1.28	−1.28	0.75	0.75
		Validation	0.59	0.59	0.64	0.64	−5.56	−5.56	0.69	0.69
	Sherpur	Calibration	0.65	0.86	0.59	0.38	−8.38	0.17	0.85	0.87
		Validation	0.16	0.67	0.92	0.57	−23.13	−12.26	0.79	0.82

reach is less that that represented by the storage time constants of the routing equation. However, if the amount of water transferred from a river reach to a wetland is offset due to higher storage effects of a river reach, then such a difference in simulated river stages between SWAT and SWATrw might not be seen.

For both models, performance for the validation period is lower than that achieved for the calibration period. According to the criteria of Moriasi et al. (2007) all the gauging stations except the lowest (Sherpur) show satisfactory simulated monthly discharge for the validation period (NSE > 0.5, RSR ≤ 0.70 and PBIAS ≤ ±55%). As discussed previously, the superior river stage simulation by SWATrw is also evident in the validation period. CRU rainfall data were used for the validation period over the Indian part of the basin since the station records used for the earlier calibration period were not available. An initial investigation shows that the average annual CRU rainfall over the Barak River basin is approximately 500 mm higher than that of IMD average annual rainfall (2443 mm) during the calibration period (2004–2010). It is not unreasonable to assume that this trend of overestimation by CRU would extend to the validation period (1990–2003). Another shortcoming of the CRU rainfall data is its contradictory annual rainfall trend compared to findings of Deka et al. (2013). These authors showed, using observed monthly rainfall data for the period 1901–2010, that the Barak River Basin has experienced a significant decreasing trend in annual rainfall that was particularly pronounced in the last three decades. CRU data suggest a reverse trend for the period 1990–2010. Overestimation of rainfall by the CRU data may therefore be responsible for the overestimated stream flows in the Kushiyara River at Sheola and in the Surma River at Kanairghat during the validation period (Fig. 9a and b and Table 5). This argument is equally applicable to the downstream Sherpur gauging station on the Kushiyara River. In general, the two models show very little differences in reproducing streamflows despite their dissimilar wetland-river interaction modules but SWATrw showed better skill in simulating daily river stages compared to SWAT.

3.3. Comparison of SWAT/SWATrw wetland interactions with rivers and groundwater

Comparison of SWAT and SWATrw simulations of the hydrological dynamics of haor wetlands is investigated using the Hakaluki haor wetland as a case study (Fig. 4). As discussed in Section 3.2, problems associated with the use of CRU rainfall data over the upper Indian part of the river basin for the validation period impact model performance. For this reason, assessment of wetland results is restricted to the calibration period. Since there are no observed hydrometric time series data for the Hakaluki haor, a very common situation for wetlands in this and similar regions, modelled results are evaluated using the average hydrological properties of the wetland in the dry and monsoon seasons. According to previous studies (CEGIS, 2012; Choudhury and Nishat, 2005), the total water surface area of all the beels (see Section 2.4) in the Hakaluki haor is approximately 4500 ha in the dry season and the corresponding average water depth is 2 m. In the monsoon season, the maximum water surface area of the wetland can be as large as 14000 ha at a water depth of 4.30 m Fig. 11 shows the simulated volume of wetland water storage, surface area and depth from SWAT and SWATrw. The results for SWATrw more closely agree with the actual hydrological behaviour of the wetland. The maximum wetland water surface area simulated by SWATrw was 13890 ha in the two wettest years of 2004 and 2006, which is very close to observed maximal extent (14000 ha) of the wetland. Through the seven years of the simulation period the mean value of this maximum area was 12014 ha. In the dry season the simulated wetland water surface area shrinks to between 2980 and 3475 ha (Fig. 11b). Wetland water depth simulated by the same model varies from 1.8 m in the dry season to 4.3 m (Fig. 11c) in the monsoonal season. SWAT results show consistently lower wetland water volumes, surface areas and water depths. For example, the maximum (in July 2004) wetland water storage, surface area and depth simulated by SWAT were 11320 ha-m, 9367 ha and 1.23 m, respectively whereas in each dry season the simulated wetland was absolutely empty of water. The simulated mean maximum annual water surface area and depth were 7141 ha and 0.90 m, respectively. These simulated conditions differ considerably from those reported by Choudhury and Nishat (2005).

The improved performance of SWATrw over SWAT to more closely represent hydrological conditions with Hakaluki haor is linked to more representative volume-area-depth relationships and the inclusion of more realistic wetland-river and wetland-groundwater interactions. The large underestimation of wetland water volume and therefore surface area and depth by SWAT signals two possible shortcomings of SWAT: (i) inadequate incoming flows to the wetland and/or (ii) excessive water loss from the wetland. Fig. 12a shows daily inflows to the Hakaluki haor generated by both SWAT and SWATrw for the calibration period. Inflows comprise upland runoff, interflow and, in the case of SWATrw, any exchange with the river and groundwater. Results for SWATrw show sudden and short-lived increases in inflows that are not simulated by SWAT. These inflows are the result of diverting water

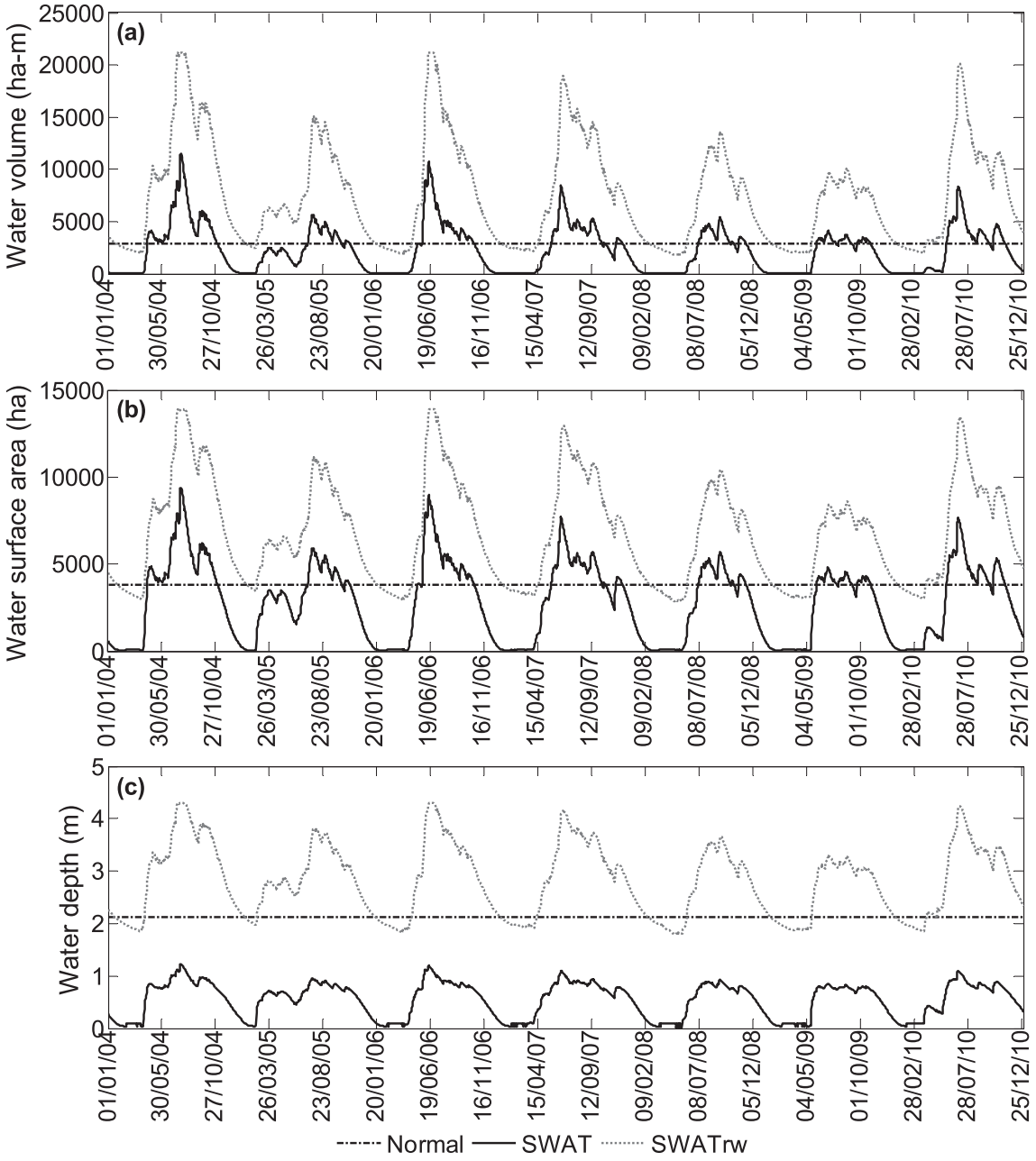

Fig. 11. Comparison of SWAT and SWATrw simulated time series of different hydrometric properties (storage, area and depth) for the Hakaluki haor wetland. The "normal" horizontal line indicates the wetland hydrometric properties at the bed level of the connecting channel.

into the wetland from the River Juri via the SWATrw connecting channel. For example, the sudden peak inflow (~140 $m^3 s^{-1}$) on 3rd May 2004 is associated with a flood event in the wetland due to gains in river stage caused by increased river discharge from the upper sub-basins (see Fig. 11b). During this event the wetland expanded by 518 ha from the initial pre-flood area of 8179 ha. Average annual mass balance analysis of the different hydrological components shows that total inflow to the wetland is 6126 ha-m (11.5%) higher in SWATrw compared to SWAT (Table 6).

Analysis of SWAT's wetland morphometric formula (Equation (3)) shows that the model tends to produce less upland inflows compared to SWATrw for any specific water storage in the wetland. Equation (3) cannot conserve the additive principle of surface area adopted in the SWAT model. This principle entails that the total surface area of a sub-basin may be fractioned into a number of spatial units (HRUs, see Section 2.1) but the combined area of these units must be equal to the sub-basin's area. Accordingly, since a wetland is fractioned among the HRUs within a sub-basin (see Section 2.2), the sum of any specific wetland property (e.g. wetland water volume and surface area) across all the HRUs in a sub-basin must be equal to the full-scale (i.e. sub-basin-scale) value of the property. Mathematically it can be proved that Equation (3) cannot preserve the areal conservation principle and instead it overestimates wetland water surface area for a given volume of water (see Annex A). An overestimated wetland water surface area reduces its upland catchment area and thus upland inflows are also reduced (see Equation (2)). On the other hand, the three vertical hydrological processes (precipitation, evaporation and seepage) that are quantified based on wetland water surface area, are likely to be overestimated by SWAT. However, this overestimating trend

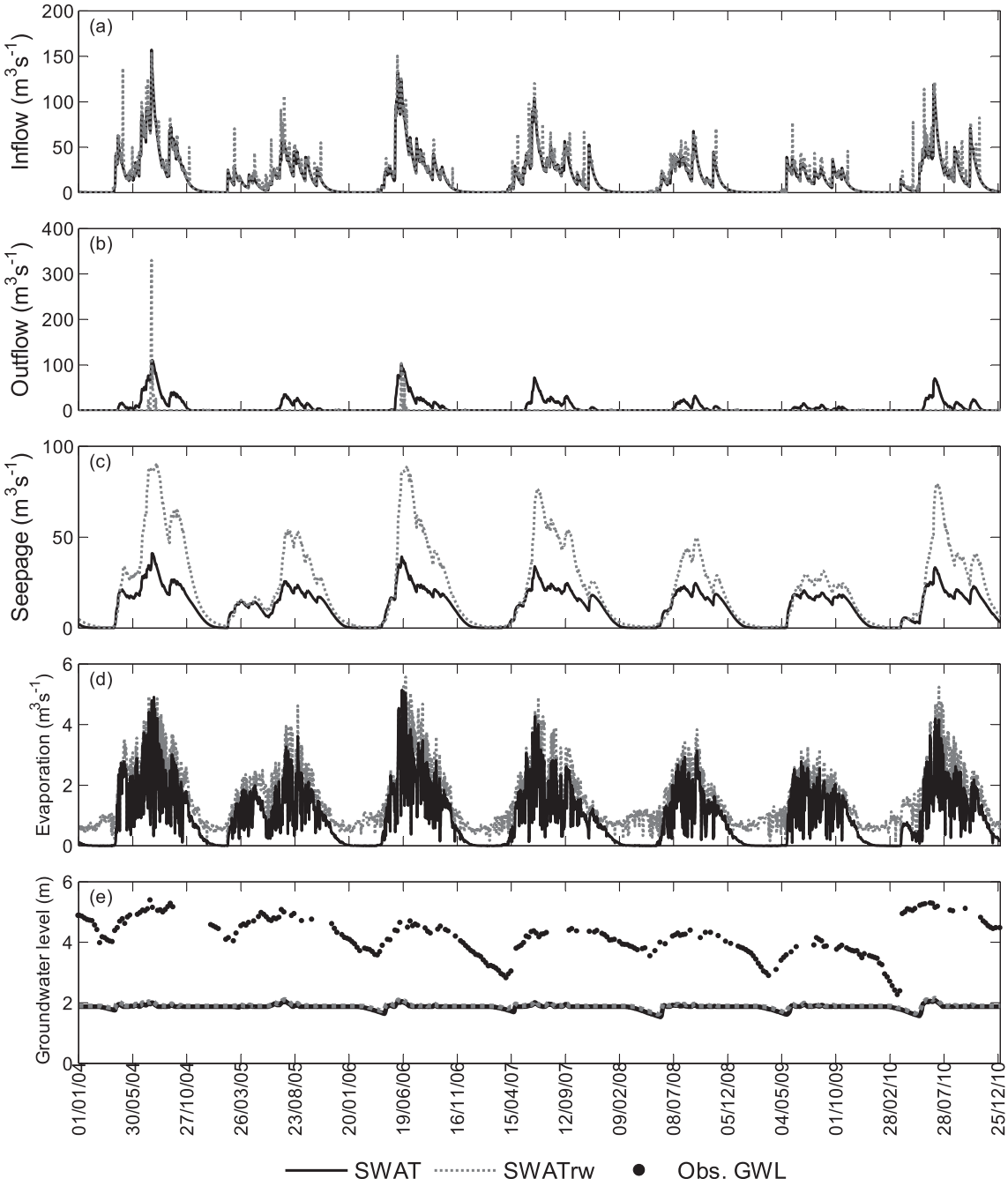

Fig. 12. Comparison of SWAT and SWATrw simulated daily inflows to (a), and surface outflows (wetland spillage - b), seepage (c) and evaporation (d) from the Hakaluki haor wetland. Simulated groundwater level (GWL) for the dominant HRU (Land use: Rice; soil: Cambisols, slope: 0–2%) is also compared with the observed values (e). The inflow comprises upland runoff, interflow and in the case of SWATrw, any inflows with the river and groundwater. The surface outflow and seepage from a wetland are destined for the adjacent river and aquifer, respectively. GWL is referenced from the wetland bottom i.e. wetland bottom is set to zero datum and observed GWLs is obtained from an observation well approximately five km from the deepest point in the wetland. The "normal" horizontal line indicates the wetland hydrometric properties at the bed level of the connecting channel.

for these processes is not apparent in results for the Hakaluki haor wetland (Fig. 12c, d and Table 6), since SWATrw consistently simulates larger volumes of water, and thus larger water surface area, compared to SWAT throughout the entire simulation period (Fig. 11a and b).

According to Fig. 12b, the wetland simulated by SWAT spills throughout the entire monsoon and post-monsoon seasons in all year of the simulation period. The annual maximum outflow ranges between 7 and 110 $m^3 s^{-1}$. In contrast, wetland outflows from the SWATrw model only occur during the monsoon season of 2004 and 2006. Peak outflows are of the range 110–330 $m^3 s^{-1}$ and are less prolonged compared to SWAT. On average SWAT produces annual outflows which are 15 times larger than those simulated by SWATrw (Table 6). In SWAT, the wetland water level is above the normal volume level (threshold value required to initiate wetland spills) during the monsoon and post-mosnsoon (Fig. 11a) and so continuously discharges to the river. Within SWATrw, although the wetland water level does exceed the normal level for a considerable

Table 6
Annual average values of simulated hydrological components of the Hakaluki haor wetland.

Hydrological components	SL. NO.	SWAT	SWATrw
Precipitaiton (ha-m yr^{-1})	(i)	13994	18609
Evaporation (ha-m yr^{-1})	(ii)	3034	4718
Seepage from wetland (ha-m yr^{-1})	(iii)	37207	71222
Inflows (ha-m yr^{-1}) from upland, river and aquifer[a]	(iv)	53001	59127
Outflows (wetland spillage) to river (ha-m yr^{-1})	(v)	26743	1757
Balance (ha-m yr^{-1}) = (i) + (iv) − (ii) − (iii) − (v)		10	39

[a] SWAT wetland receives only upland inflows (surface runoff and interflow) but SWATrw wetland receives all the three inflows.

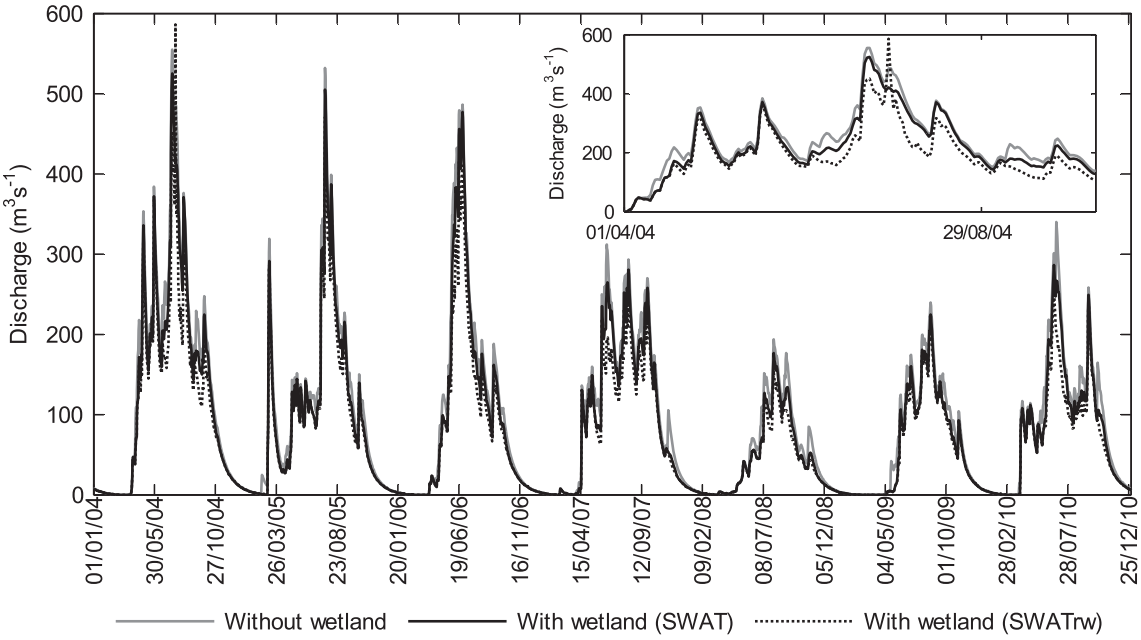

Fig. 13. Influence of the Hakaluki haor wetland on downstream river discharges simulated by SWAT and SWATrw. The inset shows a detailed view of the time series for 2004.

time in most years (Fig. 11c), flows to the river are, as discussed, restricted. This is because for most of the time the head gradient between river and wetland was such that water was simulated as entering rather than leaving the wetland. Differences in the way interactions between rivers and wetlands within the two models clearly impacts river outflows (Fig. 13).

As discussed in Section 2.2, SWAT adopts a very simple GW model where any recharge from the upper soil profile of an HRU is homogeneously accommodated in the underlying aquifer reservoir. In addition, since HRUs within a sub-basin are isolated from each other they do not exchange mass. Therefore, simulated horizontal GWLs are just an approximation of reality whereas natural GWL follows a curvilinear phreatic line while interacting with wetlands and rivers. Fig. 12e shows simulated GWLs from both SWAT and SWATrw for the largest HRU (Area = 30448 ha; land use: Rice; soil: Cambisols, slope: 0–2%) in the sub-basin containing the Hakaluki haor. This HRU has the same properties as the area around the groundwater observation well. Observed GWL from this well that are referenced with respect to the wetland bed are also shown. The groundwater observation well from which these data were acquired is approximately 5 km away from the deepest point of the wetland and the elevation of the ground surface at the well site is 7 m above the wetland's deepest point. The two models produce very similar GWL results although they are slightly higher (less than 0.05 m) for SWATrw (Fig. 12e). Clearly and expectedly, HRU averaged GWLs do not reflect the actual fluctuations of daily GWLs in a year which range from 2 m in the dry season to 5 m in the monsoon season. On the other hand, through the calibration period, simulated GWL fluctuates within a range of 1.6–1.8 m above the wetland's deepest point at the end of the dry season to a range of 2.0–2.1 m during June–July. One of the potential reasons for this limitation may be that both models assume that any change in aquifer water level due to recharge or discharge during a time step is uniform throughout the entire areal extent (equalled to HRU area) of the aquifer. This approach ignores the influence of local factors surrounding an observation well. Where groundwater flow is dominated by its horizontal component frictional head loss can be an important factor in GWL fluctuations. For the present study, the fluctuations in observed GWLs might be affected by local groundwater drawdowns originated after shallow tube well (STW) operations during the dry season. Neither of the models is able to replicate such local drawdown effects on GWLs.

Since the falling wetland water levels (Fig. 11c) after the monsoonal peaks gradually approach an equilibrium condition with the lower aquifer water levels (Fig. 12e) until the beginning of the next pre-monsoon season, SWATrw always retains some water in the wetland due to a slower downward seepage rate. The slight decline in wetland water level (Fig. 11c) during the dry season is controlled by evaporation (mean rate = 6 ha-m/day, see also Fig. 12d) and seepage (mean rate = 37 ha-m/day). However, the dry conditions within the wetland between December and April that are simulated by SWAT lead to the elimination of evaporation and seepage at this time (Fig. 12c and d). Despite reproducing almost similar GWL, SWAT was not able to simulate the actual hydrological

characteristics of the wetland since it completely ignores the principles of hydraulics for modelling wetland-groundwater interaction. The hydraulic gradient independent groundwater scheme of SWAT allows a wetland to seep water at a constant rate until it is empty. This results in the complete drying out of the Hakaluki haor that is not experienced in reality and which SWATrw avoids by preventing unrealistic wetland water loss through seepage.

Annual analysis of hydrological components shows that the SWATrw-simulated Hakaluki haor annually receives 10741 ha-m more water as inflow compared to SWAT. This mainly comes from additional direct precipitation falling on the larger wetland and from the over flowing river. The ratios of three average annual wetland outflows (evaporation, seepage and spilling) are 1:11:8 and 3:46:1 for SWAT and SWATrw respectively. This demonstrates a considerable change in the distribution of wetland seepage and spilling between the two models.

4. Summary and conclusions

The SWATrw model addresses two crucial issues in modelling water dynamics of depressional riparian wetlands with SWAT: (i) the unrealistic representation of real world wetland morphometric (volume-area-depth) relationships and (ii) the unidirectional interaction of wetlands with rivers and groundwater/aquifers. The SWATrw model replaces SWAT's wetland morphometric algorithm with the more robust and tested H-K wetland geometric formula. Wetland-river and wetland-groundwater interactions are restructured based on the principles of hydraulics without violating the mass conservation law. Therefore, the SWATrw model is more physics-based concerning the representation of the direction of wetland interactions with other water bodies (rivers and aquifers) and in the quantification of these interactions.

Both the SWAT and SWATrw models were satisfactorily calibrated (2004–2010) for the transboundary Barak-Kushiyara River Basin (Bangladesh and India) and the riparian Hakaluki haor wetland. However, using CRU rainfall data rather than station-based observations impacted model performance during the validation period (1990–2003). Comparison of SWAT and SWATrw performance provides the following major results:

(i) Both models were equally able to reproduce the volume-area relationship of the Hakaluki haor wetland but SWATrw more closely represents the volume-depth relationship. This is because the proposed volume-depth relationship by Liu et al. (2008) for SWAT is site specific and restricts its generalised use.

(ii) SWATrw-simulated time series of different wetland hydrometric properties (water storage, surface area and depth) agreed reasonably well with the seasonal behaviour of the Hakaluki haor wetland. However, the SWAT model consistently underestimated these wetland properties for all seasons. SWAT results suggested that the wetland contained no water in the dry season which is contradictory to the reported presence of water as much as 2 m deep at this time of year. The consistent downward seepage simulated by the hydraulic head independent SWAT wetland module was the prime cause of this limitation.

(iii) The hydraulic gradient-based wetland-river interaction in SWATrw was able to capture flash floods in the haor wetlands during pre-monsoon season due to over spilling of adjacent rivers. SWAT lacks such capability and wetlands only contribute water to rivers rather than also receiving inflows from them.

(iv) Of the three processes (evaporation, seepage and spilling) through which a wetland can lose water, the last two were dominant (56% and 40% of average annual wetland outflows) in SWAT for the Hakaluki haor whereas in SWATrw seepage into the aquifer alone contributed 92% of annual outflows. Despite simulating higher water levels in the River Juri compared to the wetland, SWAT unrealistically spilt more wetland water to the river. This was not seen in the results for the SWATrw model.

(v) SWAT's wetland morphometric formula cannot conserve the additive principle of surface area (i.e. the sum of all HRU-scaled constituent wetland water surface areas within a sub-basin produces a larger wetland than the actual value at the sub-basin scale). Therefore, hydrological processes affected by wetland water surface area (precipitation, evaporation, seepage, upland inflows) are inappropriately modelled by SWAT. SWATrw addresses this limitation.

More realistic modelling of wetlands, now available using SWATrw, could have potential benefits to other studies of the Barak-Kushiyara River Basin involving water quality, fisheries and conservation actions. The SWATrw model could, however, be further improved by incorporating an on-channel wetland option in addition to the current off-channel wetland. In floodplain environments such as those within the Barak-Kushiyara River Basin, it is likely that some rivers directly traverse wetlands. The absence of hydrometric time series for the wetland (storage, area and depth) remains a major limitation of this study, a factor that is common in many wetland studies (Hollis and Thompson, 1998). Both the SWAT and SWATrw models were, however, evaluated using river discharge and stage and previously reported seasonal variations in the hydrological characteristics of the Hakaluki haor wetland. The sediment and nutrients processes of SWAT were not modified in SWATrw. Future developments could adapt the current simulation of these processes to improve the representation of wetland effects upon water chemistry and sediment fluxes.

Acknowledgements

This research was supported by the UCL Ted Hollis Scholarship in Wetland Hydrology and Conservation. We thank the anonymous reviewers for their constructive comments and suggestions in improving the quality of the paper.

Annex-A. Proof of SWAT's inability to preserve the areal conservation principle

For “n” number of HRUs within a sub-basin, Equation (A.1) can be derived from Equation (3) based on the areal conservation principle:

$$\frac{A^{*}_{wet}}{A_{wet}} = \left(\frac{S_{wet,1}}{S_{wet}}\right)^{\alpha} + \left(\frac{S_{wet,2}}{S_{wet}}\right)^{\alpha} + \left(\frac{S_{wet,3}}{S_{wet}}\right)^{\alpha} + \cdots\cdots\cdots + \left(\frac{S_{wet,n}}{S_{wet}}\right)^{\alpha} \quad (A.1)$$

$$S_{wet} = S_{wet,1} + S_{wet,2} + S_{wet,3} + \cdots\cdots\cdots + S_{wet,n} \quad (A.2)$$

where A^{*}_{wet} indicates the sub-basin-scale total wetland water surface area estimated by summing HRU-scale fractioned wetland areas which is estimated from Equation (3) for known wetland water storage (S) in each HRU. SWAT applies the value of the scale factor β (see Equation (3)) derived from sub-basin-scale wetland properties (the user specified wetland water volume and surface area at maximum and normal levels) to each of the smaller HRU-scale wetland units in the sub-basin. Depending on the nature of

the shape factor α in Equation (A.1), the following relationships can be established:

$$A^*_{wet} = A_{wet} \quad if\ \alpha = 1 \tag{A.3a}$$

$$A^*_{wet} > A_{wet} \quad if\ \alpha < 1 \tag{A.3b}$$

$$A^*_{wet} < A_{wet} \quad if\ \alpha > 1 \tag{A.3c}$$

Therefore unless the value of shape factor (α) is unity (Equation (A.3a)), the wetland algorithm used in SWAT will overestimate the wetland water surface area for a shape factor value of less than unity (Equation (A.3b)) and underestimate the areas if the shape factor is larger than unity (Equation (A.3c)). In the current SWAT model the maximum value of the shape factor is 0.9 and for the Hakaluki haor the estimated shape factor was found to be 0.65. Consequently, for a given volume of water stored in a wetland, the surface area estimated by SWAT would be unrealistically high and exceed that estimated by SWATrw, which does not suffer from this limitation.

References

Arnold, J.G., Allen, P.M., Bernhardt, G., 1993. A comprehensive surface-groundwater flow model. J. Hydrol. 142, 47–69. http://dx.doi.org/10.1016/0022-1694(93)90004-S.

Arnold, J.G., Allen, P.M., Volk, M., Williams, J.R., Bosch, D.D., 2010a. Assessment of different representation of spatial variability on SWAT model performance. Trans. ASABE 53, 1433–1443.

Arnold, J.G., Gassman, P.W., White, M.J., 2010b. New developments in the SWAT ecohydrology model. In: 21st Century Watershed Technology: Improving Water Quality and Environment. ASABE.

Arnold, J.G., Srinivasan, R., Muttiah, R.S., Williams, J.R., 1998. Large area hydrologic modeling and assessment part I: model development. J. Am. Water Resour. Assoc. 34, 73–89.

ASCE, 1993. Criteria for evaluation of watershed models. J. Irrig. Drain. Eng. 119, 429–442.

Baker, C., Lawrence, R., Montagne, C., Patten, D., 2006. Mapping wetlands and riparian areas using LANDSAT ETM+ imagery and decision-tree-based models. Wetlands 26, 465–474.

Bengtson, M.L., Padmanabhan, G., 1999. A Review of Models for Investigating the Influence of Wetlands on Flooding (Fargo, ND).

Beven, K., Freer, J., 2001. Equifinality, data assimilation, and estimation in mechanistic modeling of complex environmental systems using the GLUE methodology. J. Hydrol. 249, 11–29.

Bingeman, A.K., Kouwen, N., Soulis, E.D., 2006. Validation of the hydrological processes in a hydrological model. J. Hydrol. Eng. 11, 451–463.

Bouwer, H., 2002. Artificial recharge of groundwater: hydrogeology and engineering. Hydrogeol. J. 10, 121–142.

Bullock, A., Acreman, M., 2003. The role of wetlands in the hydrological cycle. Hydrol. Earth Syst. Sci. 7, 358–389. http://dx.doi.org/10.5194/hess-7-358-2003.

BWDB, FPCO, 1993. Manu River Improvement Project, FAP6, Northeast Regional Water Management Project (Dhaka, Bangladesh).

CEGIS, 2012. Master Plan of Haor Areas, Volume I (Dhaka, Bangladesh).

Chen, H., Zhao, Y.W., 2011. Evaluating the environmental flows of China's Wolonghu wetland and land use changes using a hydrological model, a water balance model, and remote sensing. Ecol. Modell. 222, 253–260. http://dx.doi.org/10.1016/j.ecolmodel.2009.12.020.

Choudhury, G.A., Nishat, A., 2005. Hydro-meteorological Characteristics of Hakaluki Haor (Dhaka, Bangladesh).

Clilverd, H.M., Thompson, J.R., Heppell, C.M., Sayer, C.D., Axmacher, J.C., 2013. River-floodplain hydrology of an embanked lowland Chalk river and initial response to embankment removal. Hydrol. Sci. J. 58, 627–650.

Craft, C.B., Casey, W.P., 2000. Sediment and nutrient accumulation in floodplain and depressional freshwater wetlands of Georgia, USA. Wetlands 20, 323–332. http://dx.doi.org/10.1672/0277-5212(2000)020[0323:SANAIF]2.0.CO;2.

Cukier, R.I., Fortuin, C.M., Shuler, K.E., Petschek, A.G., Schaibly, J.H., 1973. Study of sensitivity of coupled reaction systems to uncertainties in rate coefficients. 1. Theory. J. Chem. Phys. 59, 3873–3878.

Cukier, R.I., Schaibly, J.H., Shuler, K.E., 1975. Study of the sensitivity of coupled reaction systems to uncertainties in rate coefficients. III. Analysis of the approximations. J. Chem. Phys. 63, 1140–1149. http://dx.doi.org/10.1063/1.1680571.

Deka, R.L., Mahanta, C., Pathak, H., Nath, K.K., Das, S., 2013. Trends and fluctuations of rainfall regime in the Brahmaputra and Barak basins of Assam, India. Theor. Appl. Climatol. 114, 61–71. http://dx.doi.org/10.1007/s00704-012-0820-x.

DHI, 2009. MIKE SHE User Documentation.

Dwivedi, R.S., Rao, B.R.M., Bhattacharya, S., 1999. Mapping wetlands of the Sundaban Delta and it's environs using ERS-1 SAR data. Int. J. Remote Sens. 20, 2235–2247.

Fan, Y., Miguez-Macho, G., 2011. A simple hydrologic framework for simulating wetlands in climate and earth system models. Clim. Dyn. 37, 253–278. http://dx.doi.org/10.1007/s00382-010-0829-8.

Feng, X.Q., Zhang, G.X., Jun Xu, Y., 2012. Simulation of hydrological processes in the Zhalong Wetland within a river basin, Northeast China. Hydrol. Earth Syst. Sci. Discuss. 9, 14035–14063. http://dx.doi.org/10.5194/hessd-9-14035-2012.

Frohn, R.C., D'Amico, E., Lane, C., Autrey, B., Rhodus, J., Liu, H., 2012. Multi-temporal sub-pixel Landsat ETM+ classification of isolated wetlands in Cuyahoga County, Ohio, USA. Wetlands 32, 289–299. http://dx.doi.org/10.1007/s13157-011-0254-8.

Golden, H.E., Lane, C.R., Amatya, D.M., Bandilla, K.W., Raanan Kiperwas, H., Knightes, C.D., Ssegane, H., 2014. Hydrologic connectivity between geographically isolated wetlands and surface water systems: a review of select modeling methods. Environ. Model. Softw. 53, 190–206. http://dx.doi.org/10.1016/j.envsoft.2013.12.004.

Gopal, B., 2013. Future of wetlands in tropical and subtropical Asia, especially in the face of climate change. Aquat. Sci. 75, 39–61. http://dx.doi.org/10.1007/s00027-011-0247-y.

Guse, B., Reusser, D.E., Fohrer, N., 2014. How to improve the representation of hydrological processes in SWAT for a lowland catchment - temporal analysis of parameter sensitivity and model performance. Hydrol. Process. 28, 2651–2670. http://dx.doi.org/10.1002/hyp.9777.

Hammer, D.E., Kadlec, R.H., 1986. A model for wetland surface water dynamics. Water Resour. Res. 22, 1951–1958.

Hansen, M.C., Defries, R.S., Townshend, J.R.G., Sohlberg, R., 2000. Global land cover classification at 1 km spatial resolution using a classification tree approach. Int. J. Remote Sens. 21, 1331–1364.

Harris, I., Jones, P.D., Osborn, T.J., Lister, D.H., 2014. Updated high-resolution grids of monthly climatic observations - the CRU TS3.10 Dataset. Int. J. Climatol. 34, 623–642. http://dx.doi.org/10.1002/joc.3711.

Harvey, K.R., Hill, G.J.E., 2001. Vegetation mapping of a tropical freshwater swamp in the Northern Territory, Australia: a comparison of aerial photography, Landsat TM and SPOT satellite imagery. Int. J. Remote Sens. 22, 2911–2925.

Hasan, M.R., Hossain, A.F.M.A., 2013. Surface water potentiality for minor irrigation expansion in haor areas of Bangladesh. Int. J. Civ. Eng. 2, 13–20.

Hattermann, F.F., Krysanova, V., Habeck, A., Bronstert, A., 2006. Integrating wetlands and riparian zones in river basin modelling. Ecol. Modell. 199, 379–392. http://dx.doi.org/10.1016/j.ecolmodel.2005.06.012.

Hattermann, F.F., Krysanova, V., Hesse, C., 2008. Modelling wetland processes in regional applications. Hydrol. Sci. J. 53, 1001–1012.

Hayashi, M., van der Kamp, G., 2000. Simple equations to represent the volume–area–depth relations of shallow wetlands in small topographic depressions. J. Hydrol. 237, 74–85. http://dx.doi.org/10.1016/S0022-1694(00)00300-0.

Heimann, D.C., Krempa, H.M., 2011. Cumulative effects of impoundments on the hydrology of riparian wetlands along the Marmaton River, West-Central Missouri, USA. Wetlands 31, 135–146. http://dx.doi.org/10.1007/s13157-010-0121-z.

Hollis, G.E., Thompson, J.R., 1998. Hydrological data for wetland management. J. Chart. Inst. Water Environ. Manag. 12, 9–17.

Islam, S.N., 2010. Threatened wetlands and ecologically sensitive ecosystems management in Bangladesh. Front. Earth Sci. China 4, 438–448. http://dx.doi.org/10.1007/s11707-010-0127-0.

Jaber, F.H., Shukla, S., 2012. MIKE SHE: model use, calibration, and validation. Trans. ASABE 55, 1479–1489.

Jaber, F.H., Shukla, S., 2005. Hydrodynamic modeling approaches for agricultural storm water impoundments. J. Irrig. Drain. Eng. 131, 307–315.

Javaheri, A., Babbar-sebens, M., 2014. On comparison of peak flow reductions, flood inundation maps, and velocity maps in evaluating effects of restored wetlands on channel flooding. Ecol. Eng. 73, 132–145.

Jhajharia, D., Dinpashoh, Y., Kahya, E., Singh, V.P., Fakheri-Fard, A., 2012. Trends in reference evapotranspiration in the humid region of northeast India. Hydrol. Process 26, 421–435. http://dx.doi.org/10.1002/hyp.8140.

Jing, L., Chen, B., 2011. Hydrological modeling of subartic wetlands: comparison between SLURP and WATFLOOD. Environ. Eng. Sci. 28, 521–533. http://dx.doi.org/10.1089/ees.2010.0277.

Johnson, W.C., Werner, B., Guntenspergen, G.R., Voldseth, R. a., Millett, B., Naugle, D.E., Tulbure, M., Carroll, R.W.H., Tracy, J., Olawsky, C., 2010. Prairie wetland complexes as landscape functional units in a changing climate. Bioscience 60, 128–140. http://dx.doi.org/10.1525/bio.2010.60.2.7.

Junk, W.J., An, S., Finlayson, C.M., Gopal, B., Květ, J., Mitchell, S. a., Mitsch, W.J., Robarts, R.D., 2013. Current state of knowledge regarding the world's wetlands and their future under global climate change: a synthesis. Aquat. Sci. 75, 151–167. http://dx.doi.org/10.1007/s00027-012-0278-z.

Kadlec, R.H., Wallace, S.D., 2009. Treatment Wetlands, Second. ed. CRC Press, Taylor & Francis Group.

Karim, F., Kinsey-Henderson, A., Wallace, J., Arthington, A.H., Pearson, R.G., 2012. Modelling wetland connectivity during overbank flooding in a tropical floodplain in north Queensland, Australia. Hydrol. Process 26, 2710–2723. http://dx.doi.org/10.1002/hyp.8364.

Kazezyılmaz-Alhan, C.M., Medina, M. a., Richardson, C.J., 2007. A wetland hydrology and water quality model incorporating surface water/groundwater interactions. Water Resour. Res. 43, 1–16. http://dx.doi.org/10.1029/2006WR005003.

Kiesel, J., Fohrer, N., Schmalz, B., White, M.J., 2010. Incorporating landscape

depressions and tile drainages of a northern German lowland catchment into a semi-distributed model. Hydrol. Process 24, 1472–1486. http://dx.doi.org/10.1002/hyp.7607.
Kite, G., 2001. Modelling the Mekong: hydrological simulation for environmental impact studies. J. Hydrol. 253, 1–13. http://dx.doi.org/10.1016/S0022-1694(01)00396-1.
Kite, G., Droogers, P., 2000. Integrated Basin Modeling (Colombo, Sri Lanka).
Kouwen, N., 2013. WATFLOOD/WATROUTE Hydrological Model Routing & Flow Forecasting System. University of Waterloo, Ontario, Canada.
Kouwen, N., 1988. WATFLOOD: a micro-computer based flood forecasting system based on real-time weather radar. Can. Water Resour. J. 13, 62–77. http://dx.doi.org/10.4296/cwrj1301062.
Krasnostein, A.L., Oldham, C.E., 2004. Predicting wetland water storage. Water Resour. Res. 40 http://dx.doi.org/10.1029/2003WR002899.
Krause, S., Bronstert, A., Zehe, E., 2007. Groundwater–surface water interactions in a North German lowland floodplain – implications for the river discharge dynamics and riparian water balance. J. Hydrol. 347, 404–417. http://dx.doi.org/10.1016/j.jhydrol.2007.09.028.
Krysanova, V., Hatterman, F., Wechsung, F., 2005. Development of the ecohydrological model SWIM for regional impact studies and vulnerability assessment. Hydrol. Process 19, 763–783.
Kulawardhana, R.W., Thenkabail, P.S., Vithanage, J., Biradar, C., Islam, M.A., Gunasinghe, S., Alankara, R., 2007. Evaluation of the wetland mapping methods using Landsat ETM+ and SRTM data. J. Spat. Hydrol. 7, 62–96.
Kushwaha, A., Jain, M.K., 2013. Hydrological simulation in a forest dominated watershed in Himalayan region using SWAT model. Water Resour. Manag. 27, 3005–3023. http://dx.doi.org/10.1007/s11269-013-0329-9.
Lehner, B., 2005. HydroSHEDS Technical Documentation. Version 1.0. Washington.
Li, M., Ma, Z., Du, J., 2010. Regional soil moisture simulation for Shaanxi Province using SWAT model validation and trend analysis. Sci. China Earth Sci. 53, 575–590. http://dx.doi.org/10.1007/s11430-010-0031-1.
Lindsay, J.B., Creed, I.F., 2005. Sensitivity of digital landscapes to artifact depressions in remotely-sensed DEMs. Photogramm. Eng. Remote Sens. 71, 1029–1036. http://dx.doi.org/10.14358/PERS.71.9.1029.
Lindsay, J.B., Creed, I.F., Beall, F.D., 2004. Drainage basin morphometrics for depressional landscapes. Water Resour. Res. 40, 1–9. http://dx.doi.org/10.1029/2004WR003322.
Liu, Y., Yang, W., Wang, X., 2008. Development of a SWAT extension module to simulate riparian wetland hydrologic processes at a watershed scale. Hydrol. Process 22, 2901–2915. http://dx.doi.org/10.1002/hyp.
Mansell, R.S., Bloom, S.A., Sun, G., 2000. A model for wetland hydrology: description and validation. Soil Sci. 165, 384–397.
Markstrom, S.L., Niswonger, R.G., Regan, R.S., Prudic, D.E., Barlow, P.M., 2008. GSFLOW—Coupled groundwater and surface-water flow model based on the integration of the precipitation-runoff modeling system (PRMS) and the modular ground-water flow model (MODFLOW-2005). In: U.S. Geological Survey Techniques and Methods. U.S. Geological Survey, Virginia, p. 240.
Martinez-Martinez, E., Nejadhashemi, A.P., Woznicki, S.A., Love, B.J., 2014. Modeling the hydrological significance of wetland restoration scenarios. J. Environ. Manage 133, 121–134. http://dx.doi.org/10.1016/j.jenvman.2013.11.046.
Maxa, M., Bolstad, P., 2009. Mapping northern wetlands with high resolution satellite images and LiDAR. Wetlands 29, 248–260.
McDonald, M.G., Harbaugh, A.W., 1988. A modular three-dimensional finite-difference ground-water flow model. In: Book 6: Modeling Techniques, in Techniques of Water Resources Investigations of the United States Geological Survey. U.S. Geological Survey, Washington.
Mendoza-Sanchez, I., Phanikumar, M.S., Niu, J., Masoner, J.R., Cozzarelli, I.M., McGuire, J.T., 2013. Quantifying wetland–aquifer interactions in a humid subtropical climate region: an integrated approach. J. Hydrol. 498, 237–253. http://dx.doi.org/10.1016/j.jhydrol.2013.06.022.
Min, J.-H., Perkins, D.B., Jawitz, J.W., 2010. Wetland-groundwater interactions in subtropical depressional wetlands. Wetlands 30, 997–1006. http://dx.doi.org/10.1007/s13157-010-0043-9.
Mishra, A., Kar, S., 2012. Modeling hydrologic processes and NPS pollution in a small watershed in subhumid subtropics using SWAT. J. Hydrol. Eng. 17, 445–454. http://dx.doi.org/10.1061/(ASCE)HE.1943-5584.0000458.
Moriasi, D.N., Arnold, J.G., Liew, M.W., Van Bingner, R.L., Harmel, R.D., Veith, T.L., 2007. Model evaluation guidelines for systematic quatification of accuracy in watershed simulations. Trans. ASABE 50, 885–900.
MPO, 1991. Description of Groundwater Model Programs (Dhaka, Bangladesh).
Murphy, P.N.C., Ogilvie, J., Connor, K., Arp, P. a., 2007. Mapping wetlands: a comparison of two different approaches for New Brunswick, Canada. Wetlands 27, 846–854. http://dx.doi.org/10.1672/0277-5212(2007)27[846:MWACOT]2.0.CO;2.
Nash, J.E., Sutcliffe, J.V., 1970. River flow forecasting through conceptual models. Part I: a discussion of principles. J. Hydrol. 10, 282–290.
Neitsch, S.L., Arnold, J.G., Kiniry, J.R., Williams, J.R., 2011. Soil and Water Assessment Tool, Theoretical Documentation, Version 2009. Grassland. Soil and Water Research, College Station.
Nilsson, K.A., Ross, M.A., Trout, K.E., 2008. Analytic method to derive wetland stage-storage relationships using GIS areas. J. Hydrol. Eng. 13, 278–282.
Nishat, B., Rahman, S.M.M., 2009. Water resources modeling of the Ganges-Brahmaputra-Meghna River Basins using satellite remote sensing data. J. Am. Water Resour. Assoc. 45, 1313–1327. http://dx.doi.org/10.1111/j.1752-1688.2009.00374.x.
Nyarko, B.K., 2007. Floodplain Wetland-river Flow Synergy in the White Volta River Basin, Ghana.
Ogawa, H., Male, J.W., 1986. Simulating the flood mitigation role of wetlands. J. Water Resour. Plan. Manag. 112, 114–128. http://dx.doi.org/10.1061/(ASCE)0733-9496(1986)112:1(114).
Oka, T., Iguchi, M., Ahmed, S.M.U., Bala, S.K., 2013. Numerical Simulation of Flood Lake Behavior in Northeastern Bangladesh [WWW Document]. URL. http://www.hydro-soft.co.jp/image/report/iguchimk/iguchimk04.pdf.
Pfannerstill, M., Guse, B., Reusser, D., Fohrer, N., 2015. Process verification of a hydrological model using a temporal parameter sensitivity analysis. Hydrol. Earth Syst. Sci. 19, 4365–4376. http://dx.doi.org/10.5194/hess-19-4365-2015.
Phan, D.B., Wu, C.C., Hsieh, S.C., 2011. Impact of climate change on stream discharge and sediment yield in Northern Viet Nam. Water Resour. 38, 827–836. http://dx.doi.org/10.1134/S0097807811060133.
Powell, S.J., Letcher, R.A., Croke, B.F.W., 2008. Modelling floodplain inundation for environmental flows: Gwydir wetlands, Australia. Ecol. Modell. 211, 350–362. http://dx.doi.org/10.1016/j.ecolmodel.2007.09.013.
Pyzoha, J.E., Callahan, T.J., Sun, G., Trettin, C.C., Miwa, M., 2008. A conceptual hydrologic model for a forested Carolina bay depressional wetland on the Coastal Plain of South Carolina, USA. Hydrol. Process 22, 2689–2698. http://dx.doi.org/10.1002/hyp.
Rahman, M.M., Lin, Z., Jia, X., Steele, D.D., DeSutter, T.M., 2014. Impact of subsurface drainage on streamflows in the Red River of the North basin. J. Hydrol. 511, 474–483. http://dx.doi.org/10.1016/j.jhydrol.2014.01.070.
Refsgaard, J.C., 1996. Terminology, modelling protocol and classification of hydrological model codes. In: Abott, M.B., Refsgaard, J.C. (Eds.), Distributed Hydrological Modelling. Springer, Netherlands, pp. 17–39.
Restrepo, J.I., Montoya, A.M., Obeysekera, J., 1998. A wetland simulation module for the MODFLOW ground water model. Groundwater 36, 764–770.
Reusser, D.E., Buytaert, W., Zehe, E., 2011. Temporal dynamics of model parameter sensitivity for computationally expensive models with the Fourier amplitude sensitivity test. Water Resour. Res. 47 http://dx.doi.org/10.1029/2010WR009947.
Reusser, D.E., Zehe, E., 2011. Inferring model structural deficits by analyzing temporal dynamics of model performance and parameter sensitivity. Water Resour. Res. 47, 1–15. http://dx.doi.org/10.1029/2010WR009946.
Shamsudduha, M., 2010. Groundwater Dynamics and Arsenic Mobilisation in Bangladesh: a National-scale Characterisation. University College London (UCL).
Sharma, P.K., Pantuwan, G., Ingram, K.T., De Datta, S.K., 1994. Rainfed low land rice roots:soil and hydrological effects. In: Kirk, G.J.D. (Ed.), Rice Roots:nutrient and Water Use. IRRI, Laguna, Philippines, pp. 55–66.
Singh, C.R., 2010. Hydrological and Hydraulic Modelling for the Restoration and Management of Loktak Lake, Northeast India. University College London (UCL).
Singh, V., 1995. Watershed modeling. In: Singh, V.P. (Ed.), Computer Models of Watershed Hydrology. Water Resources Publications, LLC, Highlands Ranch.
Smith, R.D., Ammann, A., Bartoldus, C., Brinson, M.M., 1995. An Approach for Assessing Wetland Functions Using Hydrogeomorphic Classifications, Referene Wetlands, and Functional Indices (Washington).
Sophocleous, M., 2002. Interactions between groundwater and surface water: the state of the science. Hydrogeol. J. 10, 52–67.
Spruill, C.A., Workman, S.R., Taraba, J.L., 2000. Simulation of daily and monthly stream discharge from small watersheds usingtThe SWAT model. Trans. ASABE 43, 1431–1439.
Sun, G., Callahan, T., Pyzoha, J.E., Trettin, C.C., Amatya, D.M., 2004. Modeling the hydrologic processes of a depressional forested wetland in South Carolina, U.S.A. In: Altinakar, M.S., Wang, S.S.Y., Holz, K.P., Kawahara, M. (Eds.), 6th International Conf. On Hydro-Science and Engineering, pp. 331–332. Brisbane, Australia.
Sun, G., Riekerk, H., Comerford, N.B., 1998. Modeling the hydrologic impacts of forest harvesting on florida FLATWOODS. J. Am. Water Resour. Assoc. 34, 843–854.
Sun, X., Bernard-Jannin, L., Garneau, C., Volk, M., Arnold, J.G., Srinivasan, R., Sauvage, S., Sánchez-Pérez, J.M., 2015. Improved simulation of river water and groundwater exchange in an alluvial plain using the SWAT model. Hydrol. Process. http://dx.doi.org/10.1002/hyp.10575.
Thompson, J., 2004. Simulation of wetland water-level manipulation using coupled hydrological/hydraulic modeling. Phys. Geogr. 25, 39–67. http://dx.doi.org/10.2747/0272-3646.25.1.39.
Thompson, J.R., Green, A.J., Kingston, D.G., Gosling, S.N., 2013. Assessment of uncertainty in river flow projections for the Mekong River using multiple GCMs and hydrological models. J. Hydrol. 486, 1–30. http://dx.doi.org/10.1016/j.jhydrol.2013.01.029.
Thompson, J.R., Sørenson, H.R., Gavin, H., Refsgaard, A., 2004. Application of the coupled MIKE SHE/MIKE 11 modelling system to a lowland wet grassland in southeast England. J. Hydrol. 293, 151–179. http://dx.doi.org/10.1016/j.jhydrol.2004.01.017.
Townsend, P.A., Walsh, S.J., 2001. Remote sensing of forested wetlands: application of multitemporal and multispectral satellite imagery to determine plant community composition and structure in southeastern USA. Plant Ecol. 157, 129–149.
Tucker, G.E., Lancaster, S.T., Gasparini, N.M., Bras, R.L., Rybarczyk, S.M., 2001. An object-oriented framework for distributed hydrologic and geomorphic modeling using triangulated irregular networks. Comput. Geosci. 27, 959–973. http://dx.doi.org/10.1016/S0098-3004(00)00134-5.
Uddin, M.J., Mohiuddin, A.S.M., Kamal, A.T.M.M., Hossain, M.A., 2012. The Agricultural potentiality of some wetland soils under Sylhet Basin of Bangladesh.

Dhaka Univ. J. Biol. Sci. 21, 39–46. http://dx.doi.org/10.3329/dujbs.v21i1.9743.
Uddin, M.R., Wade, L.J., Pyon, J.Y., Mazid, M.A., 2009. Rooting behavior of rice cultivars under different planting methods. J. Crop Sci. Biotechol. 12, 17–24.
Vazquez-Amábile, G.G., Engel, B.A., 2005. Use of SWAT to compute groundwater table depth and streamflow in the Muscatatuck river watershed. Trans. ASABE 48, 991–1003.
Voldseth, R.A., Johnson, W.C., Gilmanov, T., Guntenspergen, G.R., Millett, B.V., 2007. Model estimation of land-use effects on water levels of northern prairie wetlands. Ecol. Appl. 17, 527–540.
Wagner, P.D., Kumar, S., Fiener, P., Schneider, K., 2011. Hydrological modeling with SWAT in a monsoon-driven environment: experience from the Western Ghats, India. Trans. ASABE 54, 1783–1790.
Walton, R., Chapman, R.S., Davis, J.E., 1996. Development and application of the wetlands dynamic water budget model. Wetlands 16, 347–357. http://dx.doi.org/10.1007/BF03161325.
Wang, X., Shang, S., Qu, Z., Liu, T., Melesse, A.M., Yang, W., 2010. Simulated wetland conservation-restoration effects on water quantity and quality at watershed scale. J. Environ. Manage 91, 1511–1525. http://dx.doi.org/10.1016/j.jenvman.2010.02.023.
Wang, X., Yang, W., Melesse, A.M., 2008. Using hydrologic equivalent wetland concept within SWAT to estimate streamflow in watersheds with numerous wetlands. Trans. ASABE 51, 55–72. http://dx.doi.org/10.13031/2013.24227.
WARPO, 2000. National Water Management Plan (NWMP) (Dhaka, Bangladesh).
Wen, L., Macdonald, R., Morrison, T., Hameed, T., Saintilan, N., Ling, J., 2013. From hydrodynamic to hydrological modelling: investigating long-term hydrological regimes of key wetlands in the Macquarie Marshes, a semi-arid lowland floodplain in Australia. J. Hydrol. 500, 45–61. http://dx.doi.org/10.1016/j.jhydrol.2013.07.015.
Wilsnack, M.M., Welter, D.E., Montoya, A.M., Rest, J.I., Obeysekera, J., 2001. Simulating flow in regional wetlands with the MODFLOW wetlands package. J. Am. Water Resour. Assoc. 37, 655–674.
Wu, K., Johnston, C.A., 2008. Hydrologic comparison between a forested and a wetland/lake dominated watershed using SWAT. Hydrol. Process 22, 1431–1442. http://dx.doi.org/10.1002/hyp.
Zhang, L., Mitsch, W.J., 2005. Modelling hydrological processes in created freshwater wetlands: an integrated system approach. Environ. Model. Softw. 20, 935–946. http://dx.doi.org/10.1016/j.envsoft.2004.03.020.